Naval Surface Warfare Center
Carderock Division
West Bethesda, MD 20817-5700

NSWCCD-80-TR-2014/007 **April 2014**

NSWCCD-83-TM-2013/41

Naval Architecture and Engineering Department

Technical Report

ACCELERATION RESPONSE MODE DECOMPOSITION FOR QUANTIFYING WAVE IMPACT LOAD IN HIGH-SPEED PLANING CRAFT

by

Michael R. Riley, The Columbia Group
Dr. Timothy W. Coats, Combatant Craft Division (83)
Heidi Murphy, Combatant Craft Division (835)

Report Documentation Page

Form Approved
OMB No. 0704-0188

1. REPORT DATE	2. REPORT TYPE	3. DATES COVERED
17 APR 2014	**Final**	**-**

4. TITLE AND SUBTITLE	5a. CONTRACT NUMBER
ACCELERATION RESPONSE MODE DECOMPOSITION FOR QUANTIFYING WAVE IMPACT LOAD IN HIGH-SPEED PLANING CRAFT	5b. GRANT NUMBER
	5c. PROGRAM ELEMENT NUMBER
6. AUTHOR(S)	5d. PROJECT NUMBER
Michael R. Riley, Dr. Timothy Coats, Heidi Murphy	5e. TASK NUMBER
	5f. WORK UNIT NUMBER
7. PERFORMING ORGANIZATION NAME(S) AND ADDRESS(ES)	8. PERFORMING ORGANIZATION REPORT NUMBER
NAVSEA Carderock Naval Surface Warfare Center Carderock Division Detachment Norfolk 2600 Tarawa Court, #303 Virginia Beach, VA 23459-3239	
9. SPONSORING/MONITORING AGENCY NAME(S) AND ADDRESS(ES)	10. SPONSOR/MONITOR'S ACRONYM(S)
	11. SPONSOR/MONITOR'S REPORT NUMBER(S)

12. DISTRIBUTION/AVAILABILITY STATEMENT

Approved for public release, distribution unlimited

13. SUPPLEMENTARY NOTES

The original document contains color images.

14. ABSTRACT

This report presents a new approach for using high-speed craft acceleration data to quantify the amplitude and duration of a wave impact load. Peak acceleration, impact duration, and the change in velocity for individual wave impacts are shown to be important parameters. The approach may be used for any naval architecture or marine engineering investigation of wave impact effects on hull structure, shock mitigating seats, equipment systems, or human comfort and performance. It applies to full-scale and model-scale data.

15. SUBJECT TERMS

16. SECURITY CLASSIFICATION OF:			17. LIMITATION OF ABSTRACT	18. NUMBER OF PAGES	19a. NAME OF RESPONSIBLE PERSON
a. REPORT	b. ABSTRACT	c. THIS PAGE			
unclassified	**unclassified**	**unclassified**	**UU**	**72**	

ACCELERATION RESPONSE MODE DECOMPOSITION FOR QUANTIFYING WAVE IMPACT LOAD IN HIGH-SPEED PLANING CRAFT

NSWCCD-80-TR-2014/007

Prepared by:

Michael Riley
Senior Naval Architect
The Columbia Group

Prepared by:

Dr. Timothy Coats
Director of Research and Development
NSWCCD Code 830X

Prepared by:

Heidi Murphy
Test Engineer, Test and Evaluation
NSWCCD Code 835

Reviewed by:

Kelly Haupt
Senior Test Engineer, Test and Evaluation
NSWCCD Code 835

Approved by:

David Pogorzelski
Branch Head, Test and Evaluation Branch
NSWCCD Code 835

Post-Release Revisions

Revision	Reviewer/ Approver	Date	Change Description	Page, Section

REPORT DOCUMENTATION PAGE

Form Approved
OMB No. 0704-0188

1. REPORT DATE (*DD/MM/YY*)	**2. REPORT TYPE**	**3. DATES COVERED** *(From - To)*
17-04-2014	Final	May 2013 to July 2013

4. TITLE AND SUBTITLE

ACCELERATION RESPONSE MODE DECOMPOSITION FOR QUANTIFYING WAVE IMPACT LOAD IN HIGH-SPEED PLANING CRAFT

5a. CONTRACT NUMBER

5b. GRANT NUMBER

5c. PROGRAM ELEMENT NUMBER

6. AUTHOR(S)

Michael R. Riley (TCG), Dr. Timothy Coats (830X),
Heidi Murphy, (835)

5d. PROJECT NUMBER

5e. TASK NUMBER

5f. WORK UNIT NUMBER

7. PERFORMING ORGANIZATION NAME(S) AND ADDRESS(ES) AND ADDRESS(ES)

NAVSEA Carderock
Naval Surface Warfare Center
Carderock Division Detachment Norfolk
2600 Tarawa Court, #303
Virginia Beach, VA 23459-3239

8. PERFORMING ORGANIZATION REPORT NUMBER

NSWCCD-80-TR-2014/007
NSWCCD-83-TM-2013/41

9. SPONSORING / MONITORING AGENCY NAME(S) AND ADDRESS(ES)

NAVSEA Carderock
Naval Surface Warfare Center
Carderock Division
9500 MacArthur Blvd
West Bethesda, MD 20817-5700

10. SPONSOR/MONITOR'S ACRONYM(S)

11. SPONSOR/MONITOR'S REPORT NUMBER(S)

12. DISTRIBUTION / AVAILABILITY STATEMENT

DISTRIBUTION STATEMENT A. Approved for public release; distribution is unlimited.

13. SUPPLEMENTARY NOTES

14. ABSTRACT

This report presents a new approach for using high-speed craft acceleration data to quantify the amplitude and duration of a wave impact load. Peak acceleration, impact duration, and the change in velocity for individual wave impacts are shown to be important parameters. The approach may be used for any naval architecture or marine engineering investigation of wave impact effects on hull structure, shock mitigating seats, equipment systems, or human comfort and performance. It applies to full-scale and model-scale data.

15. SUBJECT TERMS

Wave impact Planing craft Load Acceleration

16. SECURITY CLASSIFICATION OF:			**17. LIMITATION OF ABSTRACT**	**18. NUMBER OF PAGES**	**19a. NAME OF RESPONSIBLE PERSON**
					Dr. Timothy Coats
a. REPORT	**b. ABSTRACT**	**c. THIS PAGE**		72	**19b. TELEPHONE NUMBER**
Unclassified	Unclassified	Unclassified	See 12.		757-462-4161

Standard Form 298 (Rev. 8-98)
Prescribed by ANSI Std. Z39.18

This page intentionally left blank

Contents

Page

Figures

Page

Tables

Page

This page intentionally left blank

Administrative Information

This report was prepared by the Combatant Craft Division (Code 83) of the Naval Architecture and Engineering Department at the Naval Surface Warfare Center, Carderock Division (NSWCCD) with funding provided by Naval Surface Warfare Center, Carderock Division under the Naval Innovative Science and Engineering (NISE) Section 219 research and development program.

Acknowledgements

The authors would like to thank Dr. Jack L. Price, Director of Research, Naval Surface Warfare Center, Carderock Division for overall management of wave slam phenomenology investigations. Many individuals from the Combatant Craft Division (CCD) of Naval Surface Warfare Center Carderock contributed to earlier investigations that led to the development of this report, including Scott Petersen, Will Sokol, Donald Jacobson, Kelly Haupt, Jason Marshall, Dr. H. Neil Ganey, Jason Bautista, and Brock Aron. Mr. Dean M. Schleicher, Technical Warrant Holder for Combatant Craft and Boats, Naval Sea Systems Command, Mr. David Pogorzelski, CCD Test and Evaluation Branch Head, and Mr. Kenneth Davis, CCD Deputy Director completed in-depth reviews and provided numerous comments that improved the report. Mr. Kelly Haupt, Senior Test Engineer, CCD Test and Evaluation Branch Head, also provided valuable input related to signal processing, Fourier spectra analysis, and the use of high-pass and low-pass filters. Their combined expertise and contributions in combatant craft design and acquisition, systems integration, life-cycle management and seakeeping trials data acquisition are sincerely appreciated.

Summary

This report presents a new approach for using high-speed craft acceleration data to quantify the amplitude and duration of a wave impact load. Peak acceleration, impact duration, and the change in velocity for individual wave impacts are shown to be important parameters. The approach may be used for any naval architecture or marine engineering investigation of wave impact effects on hull structure, equipment and systems, or human comfort and performance. It applies to data recorded during full-scale seakeeping trials as well as scale-model data.

Introduction

Background

The Office of Naval Research (ONR) initiated a research and development project in 2005 to understand why acceleration values documented in historical test reports from different agencies could not be used in craft comparative analyses [1]. This situation was a result of the complex nature of collecting, processing, and analyzing acceleration data, as well as the subjectivity that existed at various stages of data processing. There were no standard approaches for quantifying wave impact events. Different analysts would quantify the same environment differently so comparable results were not available. This effort evolved under further research and development sponsorship into a pursuit to understand craft motion mechanics and wave-slam phenomenology, defined as the investigation of the phenomena associated with individual wave-slam events. It is an approach to analyzing individual wave slams to better understand the cause-and-effect physical relationships between impact loading and craft responses [2]. Successful application of this approach has resulted in the ability to analyze the response of any system at a cross section on a planing craft with the same mathematical representation of a wave impact load. The results presented in this report demonstrate this is true regardless of whether it is related to hull structural design, the ruggedness of sensitive onboard equipment, the response of shock mitigation seats, or personnel comfort and human performance.

Approach

A mathematical model of a single degree of freedom system is used to establish the relationship between the load input during a wave impact and the dynamic response at a single location on a craft (i.e., measured acceleration response). Structural mode decomposition is then presented as a rational argument for the use of low-pass filtering to extract rigid body modes of response. Since the rigid body acceleration response at a cross section of the craft is directly proportional to the net force vector acting on the craft at that cross section, the rigid body acceleration measured during the wave impact period is used to quantify the amplitude and duration of the impulsive load in units of “g” and time.

Scope

The illustrated examples in this report are based on studies of acceleration data recorded during seakeeping trials of manned and unmanned high-speed planing craft in moderate and rough seas. Figure 1 shows examples of craft in the database that weighed approximately 14,000 pounds to 116,000 pounds and had lengths that varied from 33 feet to 82 feet.

Figure 1. High-Speed Planing Craft

Wave Impact Load

The dynamic load acting on any structure is typically reported in units of force or pressure, while the response is in terms of acceleration, velocity, and/or displacement in six degrees of freedom. In rough seas the relationship between a wave impact pressure distribution and the dynamic response of the craft is very complex. This is true even if only motion in a vertical direction is considered. The vertical acceleration response at any instant in time is a function of the pressure distribution on the bottom of the craft that varies across the beam and along the length of the craft.

Studies published by Rosen and Garme [3, 4] summarize efforts on model-scale to correlate recorded pressures and rigid body acceleration responses. The results show that an inertial force computed using rigid body heave acceleration recorded during impact periods correlates well with the computed force from a pressure transducer during the same impact periods. It is not surprising that this direct relationship exists between the recorded pressure load and the recorded rigid body acceleration response. This cause and effect relationship is fundamental to the analysis method presented in this report.

Unfortunately, during full-scale trials of craft, it is prohibitively expensive to record pressure distributions on the bottom of the craft. The net vertical force at a hull cross-section of the pressure distribution at any instant in time is directly proportional to the heave acceleration response at that cross-section. The heave acceleration can be extracted from recorded acceleration data using concepts of response mode decomposition. In the absence of pressure data or force measurements, it is therefore recommended that the amplitude and duration of the rigid body heave acceleration at any location be used as a measure of the severity of a wave impact load in the vertical direction. Modal decomposition methods, explained in later sections, are used to estimate rigid body heave accelerations.

Terminology

Flexural Motion

Flexural motions in the context of this report are vibrations of structural elements adjacent to installed accelerometers. They are transient vibrations excited by wave impacts and sustained vibrations excited by operating machinery.

Modal Decomposition

The mathematical separation of an observed experimental response into its different relevant modes of response is referred to as modal decomposition.

Modal Superposition

The linear addition of relevant modes of structural response that yields the final observed response is referred to as modal superposition.

Rigid Body Motion

Rigid body motions of a craft are its absolute translations (heave, surge, and sway) and rotations (pitch, roll, and yaw) in a seaway. It is also referred to as solid body motion or global motion in some fields of study. In the context of this report, the rigid body vertical acceleration of a craft is its heave acceleration at a cross section.

Shock

The term shock is used to imply mechanical shock, as opposed to electrical shock or chemical shock. Mechanical shock is an excitation of a physical system that is characterized by suddenness and severity and usually causes significant relative displacements in a component or system [5]. The words shock-input are sometimes used synonymously with the terms severe wave impact, wave slam, or impulsive load. A wave slam subjects a craft, installed equipment items, and passengers and crew to rapid changes in rigid body acceleration and rapid changes in velocity during a finite time.

Significant Wave Height

Significant wave height is a computed statistical wave height that characterizes the height of waves from trough to crest in a given sea state condition. It is the average of the highest $1/3^{rd}$ of all wave heights ($H_{1/3}$) computed using statistical algorithms from data typically measured by a wave buoy.

Velocity Change

In this report velocity change refers to the sudden change in rigid body vertical velocity (V_v) at a cross section caused by a wave impact. It may be used synonymously with impact velocity. For example, in a free fall, the maximum velocity at the time of impact becomes zero velocity in a very short period of time. The sudden change in velocity of the falling object is therefore equal to the absolute value of the impact velocity just prior to impact. It is another measure that characterizes the severity of a sudden change in rigid body acceleration during a short period of time. The change in velocity is directly proportional to the impulsive load for constant mass.

Vertical Direction

Deck mounted accelerometers installed in full-scale trials are typically oriented so that the vertical direction of the gage is oriented normal to the deck. As shown in Figure 2, the vertical direction of the accelerometer may therefore be oriented at some angle (theta) relative to the horizon during impacts. In this report vertical means normal to a flat deck.

Wave Slam

A wave slam is a violent impact between a craft and an incident wave. A wave impact is typically considered a more general term that may infer both low severity and high severity wave encounters. Impact severity depends upon the amplitude and the duration of the sudden change in rigid body acceleration.

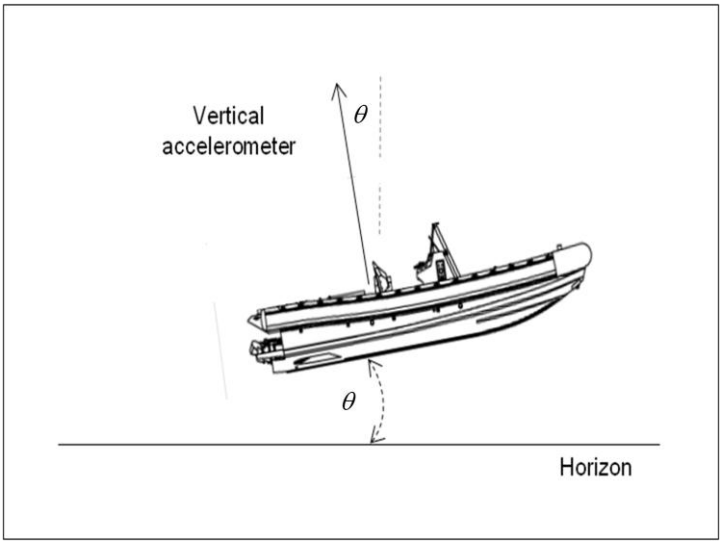

Figure 2. Orientation of Vertical Accelerometer

Wave Impact Dynamics

Typical Wave Encounters

Figure 3 shows different wave encounters measured by accelerometers for four different craft moving at different speeds in different sea states. The accelerometers were oriented vertically at the longitudinal center of gravity (LCG) of the craft. The speed-length ratio $V_K/L^{1/2}$ is a convenient parameter used in numerous historical documents because of its relationship to ocean wave celerity and the planing craft speed regimes related to ratio values of 2, 4, and 6 [6]. V_K is the average speed in knots (kn) and L is craft length in feet. The length Froude number (F_L) is another convenient parameter (in non-dimensional format) obtained by multiplying the speed ratio by 0.296 (i.e., 1.685 ft/sec/kn times $(g)^{-1/2}$).

A speed ratio of 2 (F_L = 0.59) or less represents the pre-hump condition where buoyancy forces dominate. A ratio of 4 (F_L = 1.19) is in the hump regime where the craft is beginning to

plane and both dynamic and buoyant forces participate. For a speed ratio of about 4.5 (F_L = 1.36) the craft transitions from the hump regime into the planing regime. For a speed ratio of 6 (F_L = 1.78) impact forces dominate hydrodynamic lift and buoyancy. In the upper left curve in Figure 3 the very low speed ratio of 0.13 (F_L = 0.04) is approximately equivalent to "underway but not making way". The smooth curve is characteristic of the up and down forces of gravity and buoyant forces with each passing wave. The figure illustrates that at the slower speeds the peak acceleration due to a wave encounter may be the maximum value of a smooth sinusoidal shape. As speed and sea state increase, the vertical forces due to buoyancy and gravity are still observed in the time histories, but the shapes of the responses become less smooth. Dynamic effects of higher speed wave impacts are observed as acceleration spikes followed by smooth transitions to the next wave impact spike. The shape, amplitude, and duration of the spike can depend upon numerous parameters, including significant wave height, impact angles (affected by craft trim, deadrise, and buttock), wave period, and craft speed. As speed increases into the planing regime the acceleration spikes are more pronounced as wave height increases and wave slams are experienced as violent impacts between the craft and the incident wave. The development of impact shapes is seen in Figure 3 in the upper right plot for F_L = 0.38 (1.27 speed ratio) and the lower left plot for F_L = 0.63 (speed ratio 2.12). In the planing regime the large acceleration spike shown in the lower right plot for F_L = 1.38 (4.66 speed ratio) is clearly visible. After the impact is complete the forces due to up and down wave interactions are observed as a smooth response phase associated with hydrodynamic lift forces, thrust, drag, and gravity. During a severe wave impact the force of the impact dominates the other forces.

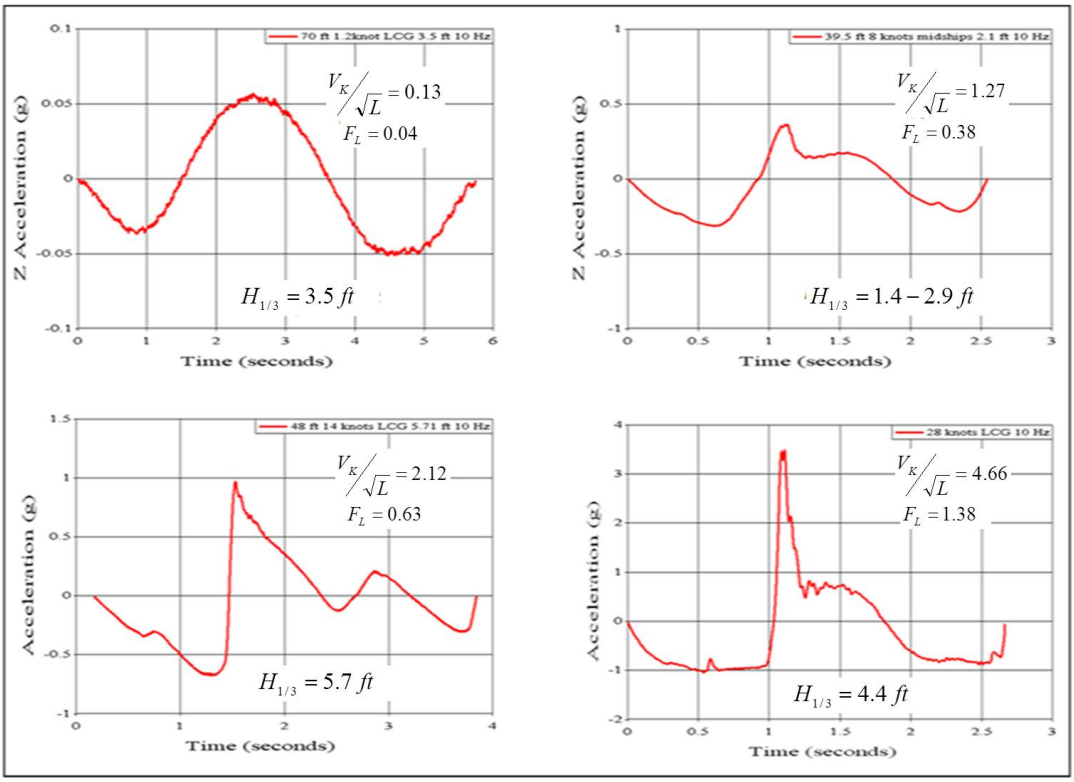

Figure 3. Slow-speed and High-speed Wave Encounters

Sequence of Events

Figure 4 illustrates the vertical sequence of events at the LCG in a typical wave slam event for a planing craft at high-speed. The upper curve shows one of the individual unfiltered acceleration responses extracted from a much longer acceleration record. The middle curve is the velocity time history obtained by integrating the acceleration curve, and the lower curve is the integral of the velocity to show the absolute vertical displacement of the craft [2].

At time A, the -0.9 g vertical acceleration indicates a condition very close to gravity free fall. The relatively constant -0.9 g from time A to time B and the linear decrease in velocity suggests that the craft is rotating downward with the stern in the water. The drop in height from time A to B is most likely a combination of heave and pitch. At time B, the craft impacts the incident wave, the velocity is at a minimum, the negative slope changes rapidly to a positive slope, and the force of the wave impact produces a sharp rise in acceleration. From time B to time C, the craft continues to move down in the water, the velocity approaches zero, and the acceleration decreases rapidly. At time C the downward displacement of the craft reaches a maximum, the instantaneous velocity is zero, and the impact event is complete. From time C to D forces due to buoyancy, hydrodynamic lift, and components of thrust and drag combine to produce a net positive acceleration. From time D to E, gravity begins to overcome the combined forces of buoyancy, hydrodynamic lift, and components of thrust and drag as another wave encounter sequence begins.

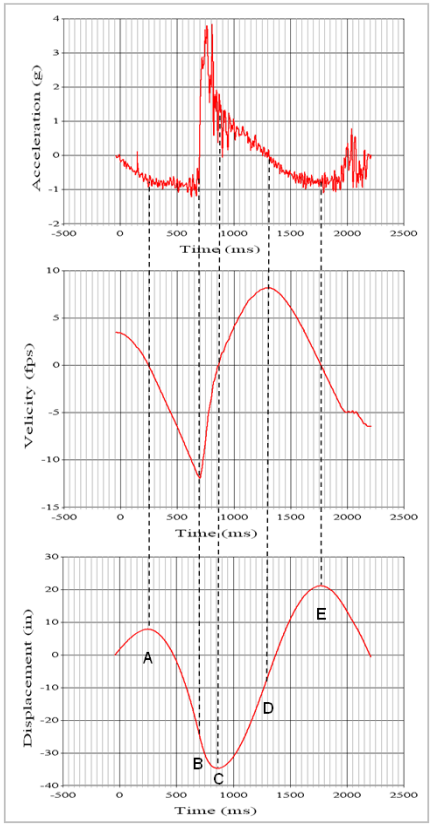

Figure 4. Wave Impact Sequence of Events

The important part of this sequence of events for quantifying impact load is the impact period from time B to time C. The rigid body component of this portion of the acceleration signal, the duration of the impact, and the positive change in velocity from the negative peak (i.e., velocity minimum) back up to zero velocity are the key parameters that characterize the severity of the impact. The importance of the rigid body acceleration content is explained in the next sections.

Types of Wave Impacts

Figures 5 through 8 illustrate three types of wave impacts observed in numerous sets of high-speed planing craft acceleration time histories [2]. Each type is unique as a result of their different sequence of events prior to the impact. All three of the types result in vertical (or near vertical) impact forces, but they exhibit varying degrees of surge (i.e., fore-aft motion) and pitch (i.e., bow-up or bow-down rotation). They are presented here to illustrate that the more severe wave impacts typically (but not always) fall within the first two categories, while the less severe impacts are typically in the third category. These observations are based on analyses of data recorded by accelerometers oriented in vertical and longitudinal (i.e., fore-aft) directions and pitch rate sensors positioned at the LCG of craft.

Type Alpha Slam

Figure 5 illustrates the Alpha slam, or type A. The upper plot shows that the vertical acceleration (red curve) is characterized by a -1 g vertical free fall and a negative longitudinal acceleration (blue curve) just before wave impact. The longitudinal positive acceleration spike seen in the blue curve indicates a force pushes forward on the LCG briefly at the beginning of the impact. The red curve in the lower plot shows a short duration negative angular acceleration spike (bow-down moment while the longitudinal acceleration spike occurs) followed rapidly by a positive angular acceleration (bow-up moment).

Most of the Type Alpha slams (except for one) are also characterized by a precursor wave encounter with a relatively long duration positive acceleration pulse that accelerates the craft upwards. This is illustrated in Figure 6 where the red curve shows there is a small perturbation at the 141 second time that indicates a low amplitude wave impact, but the majority of the response is dominated by smooth shapes due to hydrodynamic lift and buoyancy forces pushing up on the craft. The very low amplitude longitudinal acceleration (blue curve) associated with the precursor wave tends to indicate a wave skimming (or planing) wave encounter.

The data in Figures 5 and 6 suggest the following plausible description of the Type Alpha slam sequence of events. The long duration of the upward force in the precursor wave contributes to a launch and free fall sequence of events. A stern-first water entry causes a brief bow down moment, which in turn introduces the forward acceleration spike, followed by impact with the incoming wave that causes the bow-up moment and the sharp rise in vertical acceleration.

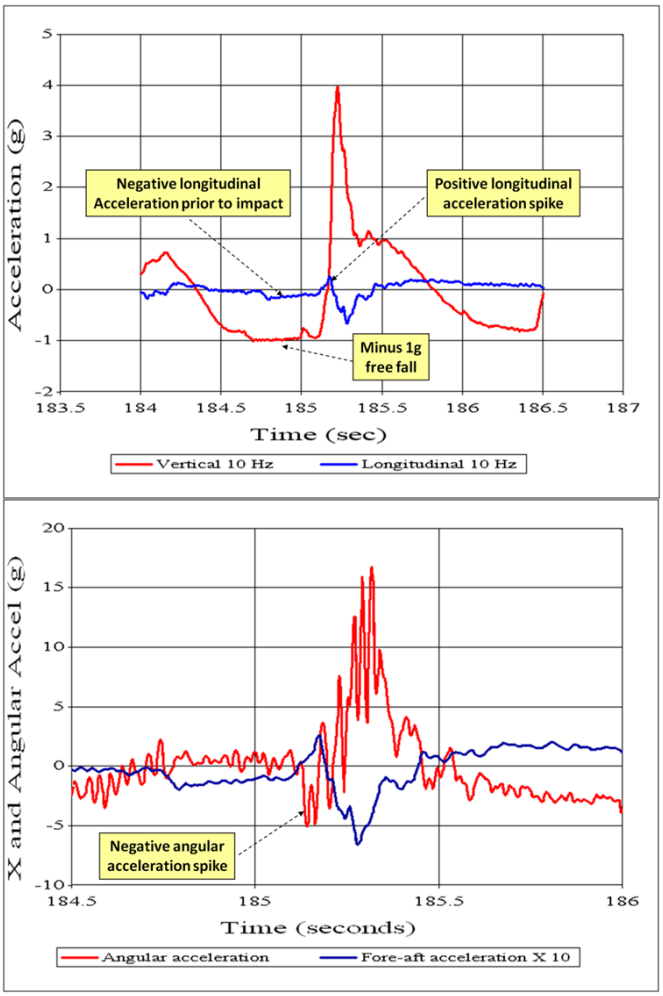

Figure 5. Type Alpha Slam Sequence of Events

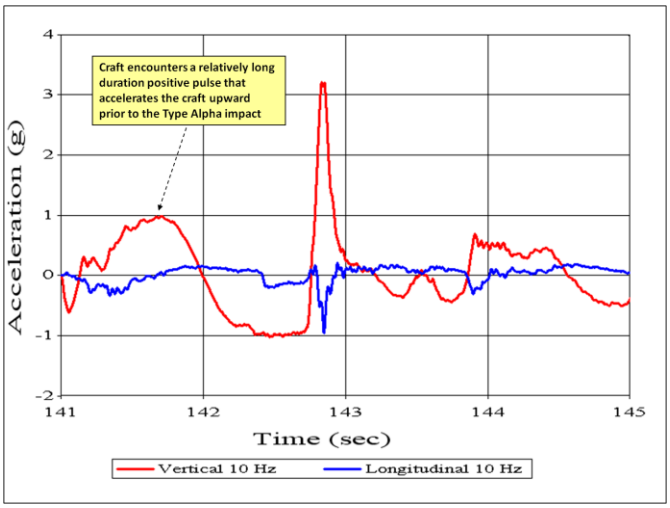

Figure 6. Type Alpha Precursor Non-Slam Event

Type Bravo Slam

The Bravo Slam, or Type B, is similar to the Alpha Slam, but there is no indication of a stern-first impact. As shown in Figure 7, the pre-impact period is characterized by a -1.0 g vertical acceleration (or close to it), a negative longitudinal acceleration, and insignificant angular acceleration (close to zero) just prior to impact. This is consistent with a sequence of events described as a free fall event with loss of thrust and little or no bow-down rotation when the keel impacts the water.

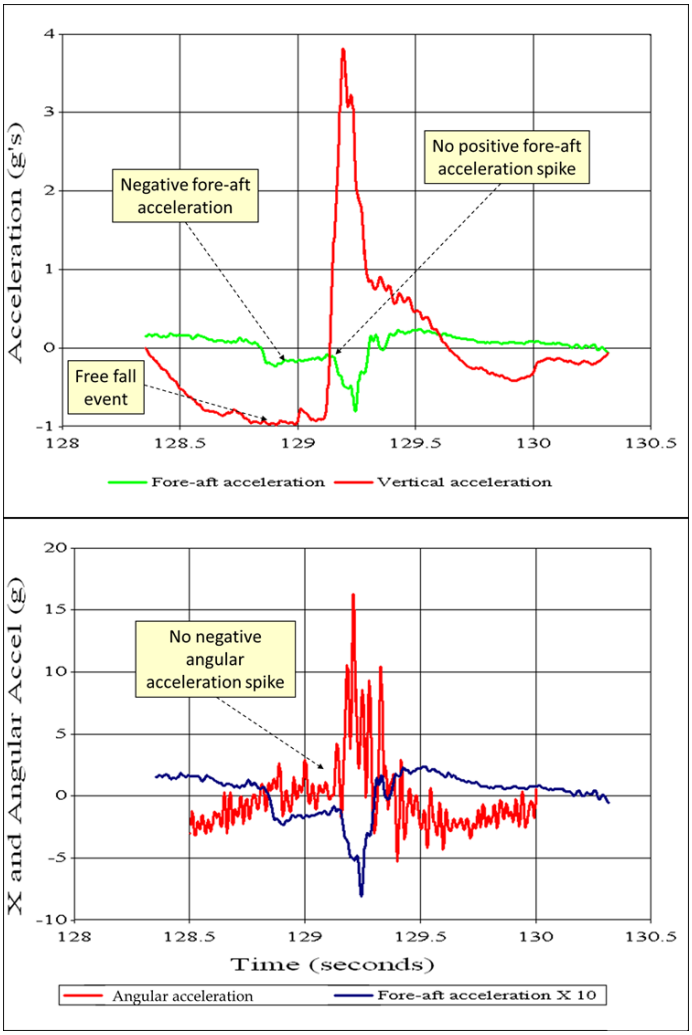

Figure 7. Type Bravo Wave Slam Sequence of Events

Type Charlie Slam

The third Type C category, or Charlie wave slam, is shown in Figure 8. In the upper plot the green curve shows there is a small positive longitudinal acceleration that indicates continuous thrust before the impact. Like the Bravo slam there is no longitudinal acceleration spike (no stern-first impact). In the lower plot the red curve shows a small negative angular rotation prior

to impact that indicates a continuous bow-down moment, which is consistent with the negative vertical acceleration in the upper red curve.

The sequence of events indicates the energy of the impact is due primarily to the relative horizontal velocity between the craft and the incident wave, and has little to do with significant vertical drop at the LCG. Prior to the slam there is forward thrust and a small bow down moment, but there is little or no free-fall event prior to the slam.

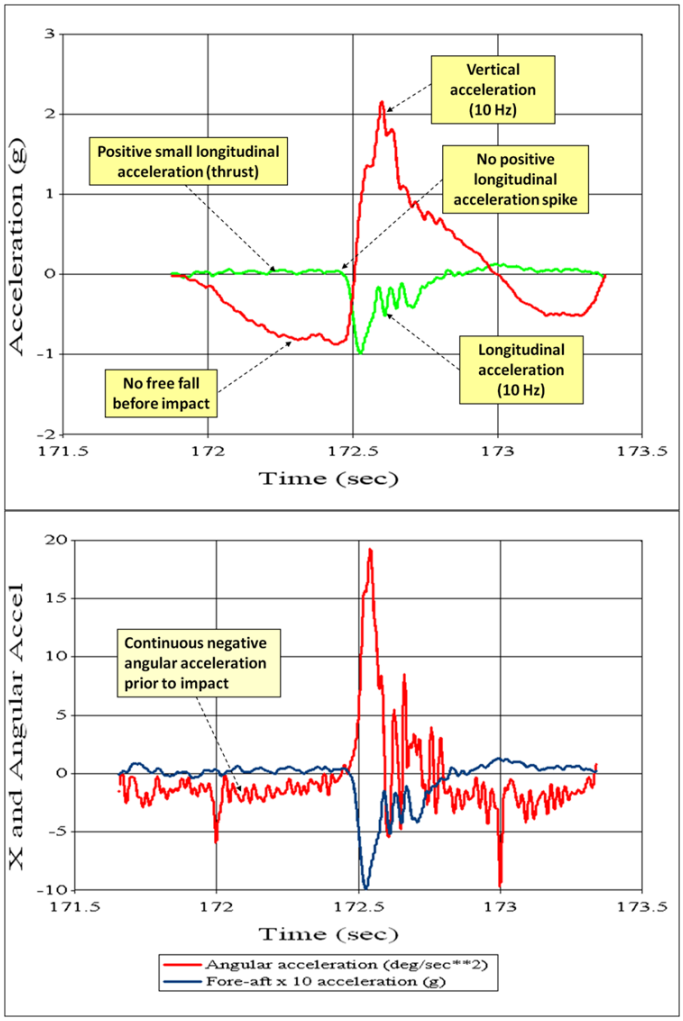

Figure 8. Type Charlie Wave Slam Sequence of Events

The Charlie slam is characterized by the lowest amplitude peak vertical accelerations (e.g., typically less than 2.5 g). Alpha and Bravo slams on the other hand have peak vertical accelerations that can be greater than 3.0 g, most likely due to the potential energy of the free fall or the rotational energy of large bow down rotations just prior to impact. The Bravo slam sequence of events has also been observed in lower amplitude impacts in the 2 g to 3 g range.

Understanding Recorded Accelerations

Acceleration Units

Figure 9 shows an example of a typical acceleration time history recorded by an accelerometer installed on the deck of a planing craft at the longitudinal center of gravity amidships and oriented vertically. It is the absolute acceleration measured relative to the surface of the earth, but it has been demeaned, resulting in an overall average value of zero. The craft was traveling into head seas at a speed in excess of 25 knots in a sea state with a significant wave height greater than 2.5 feet. Time is shown in seconds, and the measured acceleration is in ft/sec^2.

Positive acceleration is an increasing rate of change in velocity in the upward direction, and negative acceleration is an increasing rate of change in velocity in a downward direction (e.g., as in free-fall). Zero acceleration represents an instantaneous equilibrium condition where the net upward force is equal to the net downward force. The positive "spikes" on the curve are associated with individual wave impacts. At first glance, the effect of the randomness of the incident wave heights is observed as a series of spikes with amplitudes that show no discernible pattern.

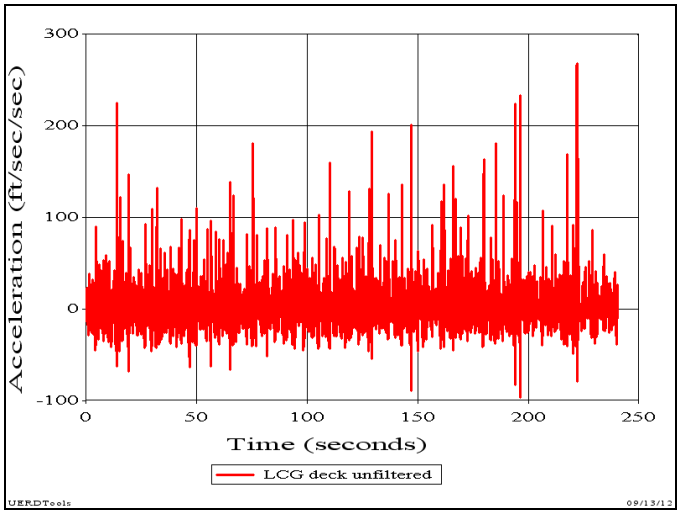

Figure 9. Typical Vertical Deck Acceleration at the LCG

Figure 10 shows the same acceleration record shown in Figure 9, but the acceleration scale has been normalized by dividing by 32.2 ft/sec^2 to yield units of g. The plotting scheme is convenient because it simplifies the visual presentation of the amplitude in multiples of the acceleration due to gravity. One g is 32.2 ft/sec^2, two g is 64.4 ft/sec^2, and so on. In the

normalized figure the larger peak accelerations are on the order of 5 to 8 times the acceleration due to gravity (i.e., 161.0 ft/sec^2 to 257.6 ft/sec^2).

Normalizing acceleration time histories by dividing by 32.2 ft/sec^2 is a common practice, but it often leads to incorrect conclusions. For example, if it is interpreted as an acceleration in units of g to be multiplied by the weight of the craft (in pounds), it leads to the incorrect assumption that the acceleration record is a measure of the applied load in pounds. This is not the case, but some authors incorrectly label the unfiltered acceleration axis in Figure 10 as a "g-load". The unfiltered peak accelerations of each wave impact in Figure 10 in units of g are not measures of wave impact load.

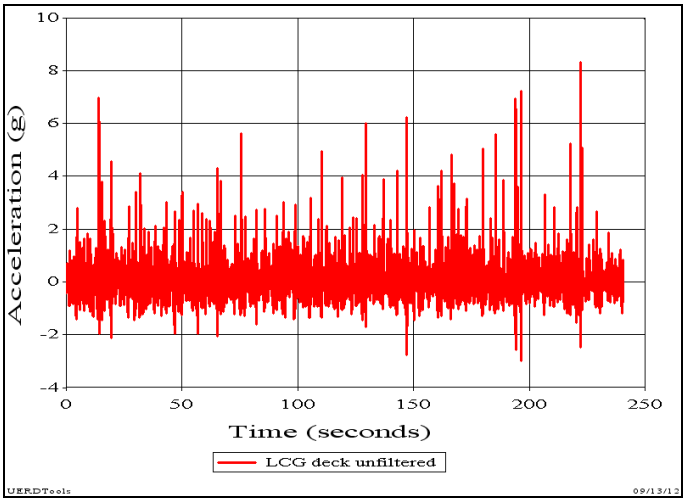

Figure 10. Acceleration in Units of g

The problem with the interpretation of the g unit arises from confusion between the concepts of rigid body mechanics and the mechanics of deformable solids. In real life there are few structures that are truly rigid. On model-scale and on full-scale the installation of accelerometers is almost always at locations with elastic properties, including wood, composites, and metals. Structures with elastic properties that are excited by dynamic loads (sometimes referred to as impulsive loads) exhibit dynamic responses that include vibrations and/or material stress waves in addition to classical rigid body modes (e.g., craft heave, surge, pitch, roll, etc.). In order to interpret an acceleration time history properly, the recorded acceleration must first be considered a response [7], before the amplitude of the input load can be estimated.

Input and Response

The steps required to properly analyze acceleration data begins with the fundamental concept of "input and response". The load of a single wave impact (i.e., the input to the craft) causes a deterministic response [2]. The word deterministic is used here because the response at a location on a craft for a single wave impact is neither random, nor is it chaotic. For a specific set of load conditions, like pulse amplitude, duration, pressure distribution, deadrise, and trim there is a unique and repeatable response (as long as permanent deformation of the structure around the accelerometer does not occur). Figure 11 illustrates the input and response concept

with a mathematical single-degree-of-freedom model oriented in the vertical direction. It is single-degree because the only mode of response motion is up-and-down displacement. There is no rotation of the mass in the model nor is there side-to-side motion. The letter "m" represents the mass of the system of interest, the letter "k" represents the stiffness of the deck and stiffeners between the mass and the point of load application, and the letter "c" represents the damping characteristics of the deck and stiffeners between the mass and the point of load application. The letter "t" signifies that the load and the response vary over time.

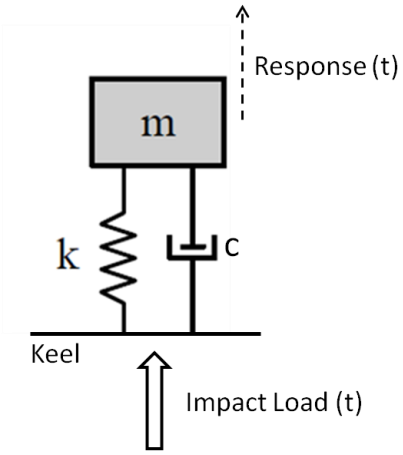

Figure 11. Single-Degree-of-Freedom Input and Response Model

A vertical accelerometer installed on the deck of a craft (or any other location) is like placing the accelerometer on top of the mass (m) in Figure 11. The hull-water interface at the keel is the point of vertical load application. The accelerometer measures the response acceleration of the mass associated with surrounding structure. As the load is applied and the keel moves upward, the mass (m) also moves upward with the motion of the keel, but as time progresses during the impact the mass also oscillates up-and-down relative to the keel due to the flexibility (i.e., stiffness-k) and material damping of the deck and stiffeners. The recorded acceleration will therefore contain two superimposed modes of response. The first mode is the vertical motion of the keel which is referred to as heave. The second mode of response of the mass is the oscillatory motion relative to the keel. These relative motions are flexural response modes of the structure referred to as deck vibrations. Wave impact durations in planing craft are typically 100 msec or more. Structural vibration response modes typically have periods of 50 msec or less. When response periods are less than the period of the input load the vibration motions will oscillate around the base input heave acceleration.

Figure 12 shows a typical vertical acceleration response measured at the LCG of a high-speed planing craft. Three separate wave impacts are observed as a very rapid change from a negative acceleration to a positive peak value. The response to each impact is observed to be a period of forced vibration above zero that occurs for a given duration. The amplitude of the forced vibration is much larger than the amplitude of the background vibration signal observed prior to each impact. The plot shows that the duration of the forced vibration response damps out prior to the next impact. This is a very important observation because it means that each impact response is not coupled to the next impact response. Therefore, each wave impact can be analyzed as a single input and response phenomenon.

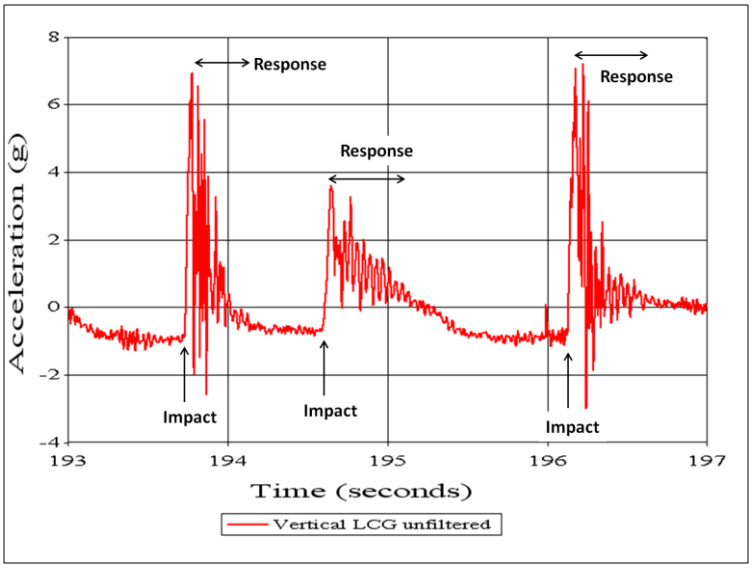

Figure 12. Acceleration Input and Response Phases

Response Mode Decomposition

Rigid Body Motion and Vibrations

The complex motion of any craft in a seaway is described by three translations (i.e., heave, surge, and sway) and three rotations (roll, pitch, and yaw) about its center of gravity. These are referred to as the six primary degrees of freedom that define the absolute motion of the craft. They are also referred to as the rigid body motion (or solid body motion) of the craft in the six degrees of freedom. The word rigid is used because it is the motion of the center of gravity of the craft as though it were a solid object not capable of internal flexure (i.e., vibrations in a dynamic environment). In a detailed analysis several degrees of freedom may be used to model the dynamic environment, but in the following paragraphs only one degree-of-freedom will be used to summarize response mode decomposition.

The concept of rigid body motion is a mathematical construct used to model forces, (including impulsive loads), momentum transfers (or energy transfers), and the dynamic response of systems. The mathematical equations of motion that describe the dynamic response of the mass (m) in Figure 11 can be written in terms of the applied force or in terms of the vertical motion of the base at the point of load application. The vertical motion at the base can be described in terms of either time histories of displacement, velocity, or acceleration, whichever is more convenient.

Unfortunately, during seakeeping trials, there are no practical force gages with which to directly measure the force of each wave impact. As a mathematical substitute, the absolute motion of the base can be used as an input to the mathematical model. Since accelerometers are typically used, the base input is conveniently described in terms of the heave acceleration, and the heave acceleration is the vertical rigid body acceleration of the craft. The vertical rigid body acceleration at a cross-section of a craft can therefore be used as a measure of the net vertical force (i.e., the load) acting at that cross-section. It is a measure of wave impact severity.

But real systems also experience internal relative motions caused by flexure of structural elements. Therefore the absolute motion recorded by an accelerometer at any point within a high-speed craft is a superposition of its rigid body acceleration at that cross-section where the gage is positioned and the relative flexural motions of structure at the gage location.

In order to extract the rigid body acceleration from the record, the recorded acceleration must be decomposed into its different modes of response. This process is referred to as modal decomposition.

One of the fundamental differences between different modes of response in a dynamic environment is the time required to complete one cycle of motion. For example, in the vertical direction the up and down cycle of heave motion is typically on the order of 0.5 seconds or more, depending upon craft speed and wave period. The up and down vibrations of structural elements are usually on the order of 0.05 seconds or less. These differences in time periods are conveniently analyzed in terms of the frequency of the dynamic response. Understanding the frequency content of an acceleration record and the source of different frequency responses is fundamentally important to characterizing the severity of a wave impact load.

Frequency Content

Accelerometers are very sensitive instruments. They measure the accelerations of all response modes, including components of the six rigid body modes and those of millimeter structural vibrations caused by wave impacts and by machinery systems. But structural vibrations are not the primary interest in rough-water seakeeping trials, so accelerometers are typically positioned at relatively stiff or massive locations, such as on deck plating directly over stiffeners or bulkheads to minimize the vibration content. But even when accelerometers are located on relatively hard spots, they are sensitive enough to record accelerations of the millimeter vibrations of plating in the vicinity of the accelerometer. Unfortunately the accelerations associated with vibrations are not small. They can be equal to or greater than rigid body heave accelerations caused by the vertical force of a wave impact at a cross-section of a craft. Figure 13 illustrates the concept that the measured vertical acceleration is a linear superposition of rigid body and flexural modes of response that have different frequencies of response [8].

During rough-water trials it is the sudden change in rigid body heave, pitch, and surge caused by wave impacts that are of primary interest. It is therefore very important to understand the flexural content (i.e., the vibration content) in a record so that rigid body accelerations can be properly characterized. Rigid body accelerations that characterize the wave slam shock pulse can be estimated by removing the flexural content using a low-pass filter in the data processing sequence [3, 4, and 10].

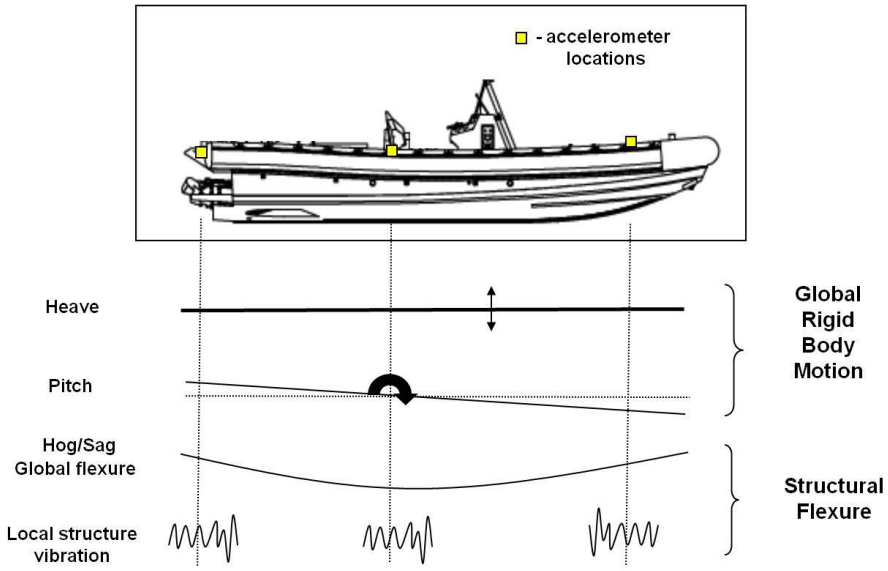

Figure 13. Different Modes of Vertical Dynamic Response

Figure 14 shows an unfiltered vertical acceleration record for one wave impact recorded at the LCG of a 36-foot craft [9]. The time increment shown is 0.02 seconds to illustrate the frequency content. The record shows that prior to the impact the craft is in a free-fall phase (i.e., -32.2 ft/sec^2, or -9.8 m/sec^2, or -1 g). A close inspection of the vibration cycles in one segment of the free-fall shows six cycles in about 0.14 seconds, which corresponds to 42.5 Hz. In other words, the structure is vibrating at a frequency of 42.5 Hz during the free-fall phase. Just after the impact, four larger amplitude cycles are observed to occur in 0.10 seconds, which corresponds to about 40 Hz. The amplitude of the forced vibration upon impact is large during two of the cycles, and varies from zero to 8 g, which will make it more difficult to determine the underlying heave acceleration. Before the forced vibrations damp out, 2 cycles are observed to occur in 0.08 seconds, which corresponds to 25 Hz. These simple observations suggest that a frequency spectrum of the acceleration record should have "humps" close to 25 Hz and close to 40 Hz.

Fourier Spectrum Analysis

A Fourier spectrum of an acceleration time history plots the amplitudes of the sinusoidal components that can be superimposed to create the time history. It is useful for identifying dominant frequency content in an acceleration record. Figure 15 is a Fourier spectrum of the acceleration record shown in Figure 14. It shows the dominant wave impact frequency to be less than 2 Hz, with lower amplitude vibration content near 25 Hz, 40 Hz, and 55 Hz. These are the frequencies of different response modes in the acceleration record. In the context of this report, separating an unfiltered acceleration record into its different modes of response is referred to as modal decomposition.

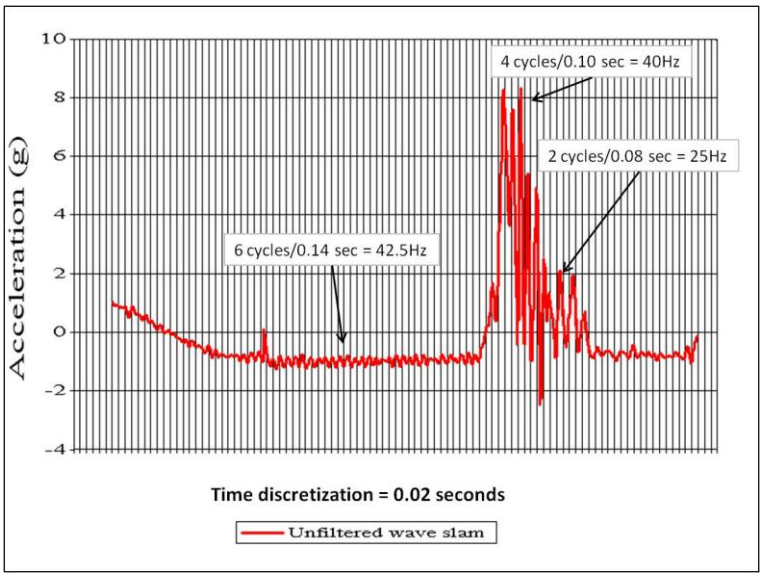

Figure 14. Frequency Content in Acceleration Record

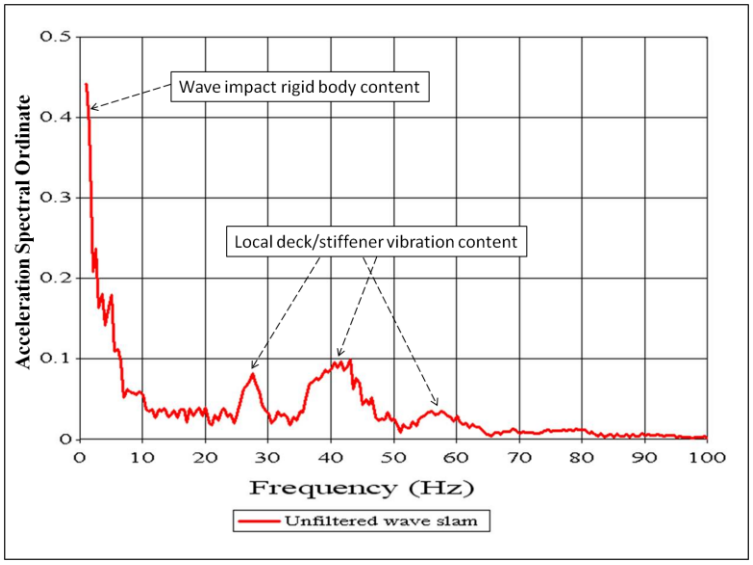

Figure 15. Fourier Spectrum of Vertical Acceleration Record

Low-Pass Filtering

Now that the overall frequency content of the acceleration record is better understood, low-pass filtering can be used to remove the vibration content in the record. Figure 16 shows the original unfiltered record (red curve) that contains both the rigid body acceleration and the acceleration of local structural vibrations with three other curves that have been low-pass filtered with different cut-off frequencies. The purpose of low-pass filtering is to remove as much as practicable the local structural vibrations, and retain as much as possible of the rigid body content, (i.e., heave acceleration). The plot shows how application of a 33 Hz, 15 Hz, and 10 Hz low-pass filter progressively eliminates the higher frequency content due to local vibrations. The

unfiltered red curve has a combined rigid body plus vibration peak acceleration of 8.25 g. The 10 Hz low-pass filtered acceleration (black with circles) provides an estimated peak rigid body acceleration of 5.31 g. At that point in time, 64% of the 8.25 g was rigid body content, and 36% was local response vibration content.

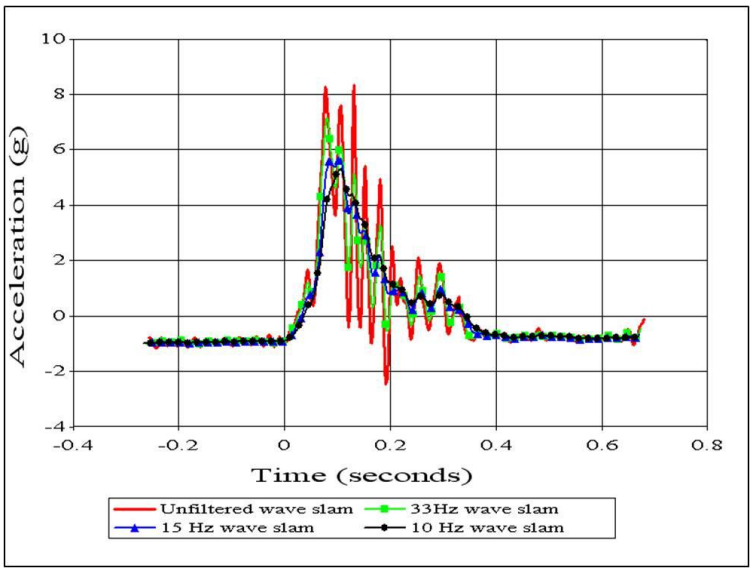

Figure 16. The Effects of Low-Pass Filtering

Figure 17 shows Fourier spectra of the four acceleration curves shown in Figure 16. They show how the filtering process successively reduces the high frequency vibration content in the record, and keeps the underlying rigid body content (i.e., the heave acceleration) at the low end of the spectrum (i.e., typically less than 2 Hz for small high-speed planing craft for speeds up to 60 knots in seas characterized by significant wave heights greater than roughly 1.6 ft).

The amplitude of the cut-off frequency of the low-pass filter affects the amplitude of the peak acceleration observed for each wave slam. For the wave slam shown in Figure 16, the unfiltered peak was 8.25 g compared to the estimated peak rigid body (heave) acceleration of 5.31 g (10 Hz filtered). These differences can be very large depending upon the gage location and the severity of the wave slam. Trials data has shown that the acceleration content due to vibrations can be on the order of 4 g to 11 g or more (depending upon accelerometer location), so the total combined acceleration amplitude may be 10 g to 18 g or more, depending upon gage location.

Another factor that will affect the amplitude of the estimated rigid body acceleration is the type of low-pass filter used. Many of the plots shown in this report were obtained using a Butterworth two-pole low-pass filter with a characteristic 12 dB per octave attenuation (6 dB per octave per pole). The original full-scale data was subjected to a Kaiser filter to estimate the vertical rigid body response (1% ripple in stop-band, 5% ripple in band-pass, stop-band frequency 20% greater than the specified band-pass frequency) [2]. Unpublished comparisons of these two filter types showed differences in estimated peak rigid body accelerations on the order of 2 percent or less. It is understood that different analysts will have access to different software

with different types of filters. The intent is therefore not to obtain exact correlation across multiple organizations, but rather to ensure that rigid body estimates are being compared, and not peak accelerations from vibrations that vary with gage location.

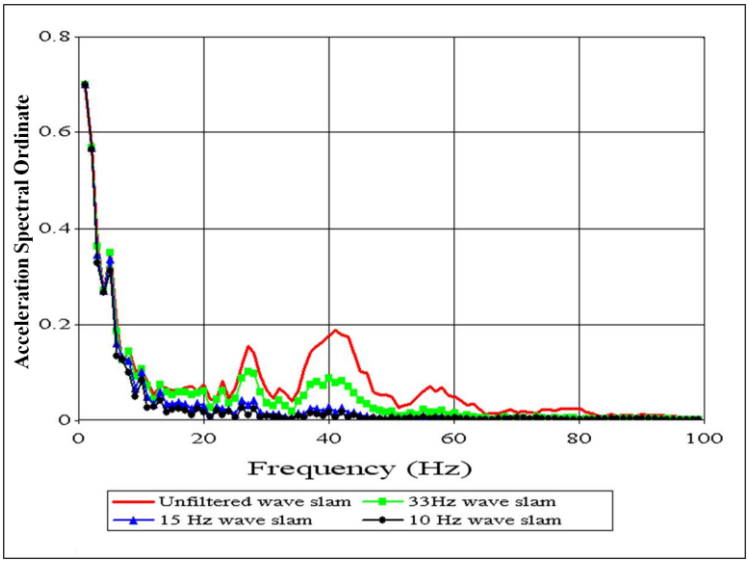

Figure 17. Fourier Spectra of Wave Impact Responses

As shown in Figure 17, experience in analyzing 21 sets of trials data for craft less than 100 feet in length indicates that the 10 Hz low-pass filter sufficiently removes local vibrations without severely affecting rigid body peak acceleration amplitudes. This confirms earlier studies that also employed 10 Hz low-pass filters when studying wave impacts on high-speed planing craft[1] [10, 11].

Low-pass filtering is basically a reverse engineering modal decomposition process used to extract the rigid body heave content from an acceleration record. The rigid body heave acceleration during the impact period is a substitute measure of the wave impact load (in any degree of freedom). It characterizes the load in units of g. Low-pass filtering should be applied to recorded acceleration data to investigate the effects of wave impact loads on hull structure, equipment, or personnel (i.e., the cause-and-effect impulse and change-in-momentum relationships).

Low-pass filtering may not be appropriate for all investigations that analyze craft acceleration data. Other unique applications may dictate selection of a different low-pass frequency or none at all. For example, in the study of the effects of different engine vibration mounts on surrounding equipment or personnel, low-pass filtering may not be appropriate at all.

Modal Decomposition

In the time domain the concept of modal decomposition is illustrated by the three plots on the left shown in Figure 18. Each plot is a 10-second segment of vertical acceleration data that

[1] Limited distribution report NAVSECNORDIV 6660-C15, March 1976.

shows six wave impacts. The accelerometer was oriented vertically and installed in the engine compartment next to an engine isolation mount, so its vibration content is much larger than typical deck locations. The red curve in the upper plot is the unfiltered vertical acceleration. The middle plot is the vertical rigid body acceleration extracted from the unfiltered acceleration by low-pass filtering. It shows three severe wave impacts where the wave slam spikes are clearly visible. The rigid body acceleration is also shown as the black curve in the upper plot to show how the vibration content "rides" on the rigid body acceleration. The bottom plot is the deck vibration content obtained by high-pass filtering. When the rigid body and the vibration responses are added it creates the original unfiltered curve shown in the upper plot.

In the frequency domain the rigid body content and the vibration content are observed as spikes and humps in the Fourier spectra shown in Figure 18. The plots on the right side are the three Fourier spectra of the three acceleration plots shown on the left side of the figure. The upper plot is the Fourier spectrum of the unfiltered acceleration record. It shows the rigid body content at frequencies less than 2 Hz and several dominant vibration modes with octave component spikes across a broad range of frequencies from roughly 30 Hz to 350 Hz. The spectrum of the rigid body content and the spectrum of the vibration content are shown to illustrate the modal decomposition process and how low-pass and high-pass filtering are used to decompose the unfiltered signal.

Figure 19 shows another set of acceleration time histories and Fourier spectra to illustrate modal decomposition for a typical deck accelerometer. The accelerometer was oriented vertically and installed on the deck above a support stiffener at the LCG of a craft. The time histories on the left show less vibration content than the data in Figure 18, but the vibration peak amplitudes are still about the same as or higher than the rigid body peak accelerations. The Fourier spectrum plots on the right side of Figure 19 show that the spectrum amplitudes of the vibration content are much less than the spectrum amplitudes of the rigid body content.

Figures 18 and 19 illustrate graphically how the phrase "shock and vibration" has evolved in the structural dynamics community. The shock load (i.e., the input) applied to real structures causes a shock response, but it is fundamentally important that the shock response of vehicles like planing craft be understood as a superposition of rigid body motions and vibrations. Once these motions are understood, impulse and momentum relationships can be used to investigate how the shock load is transmitted within the craft.

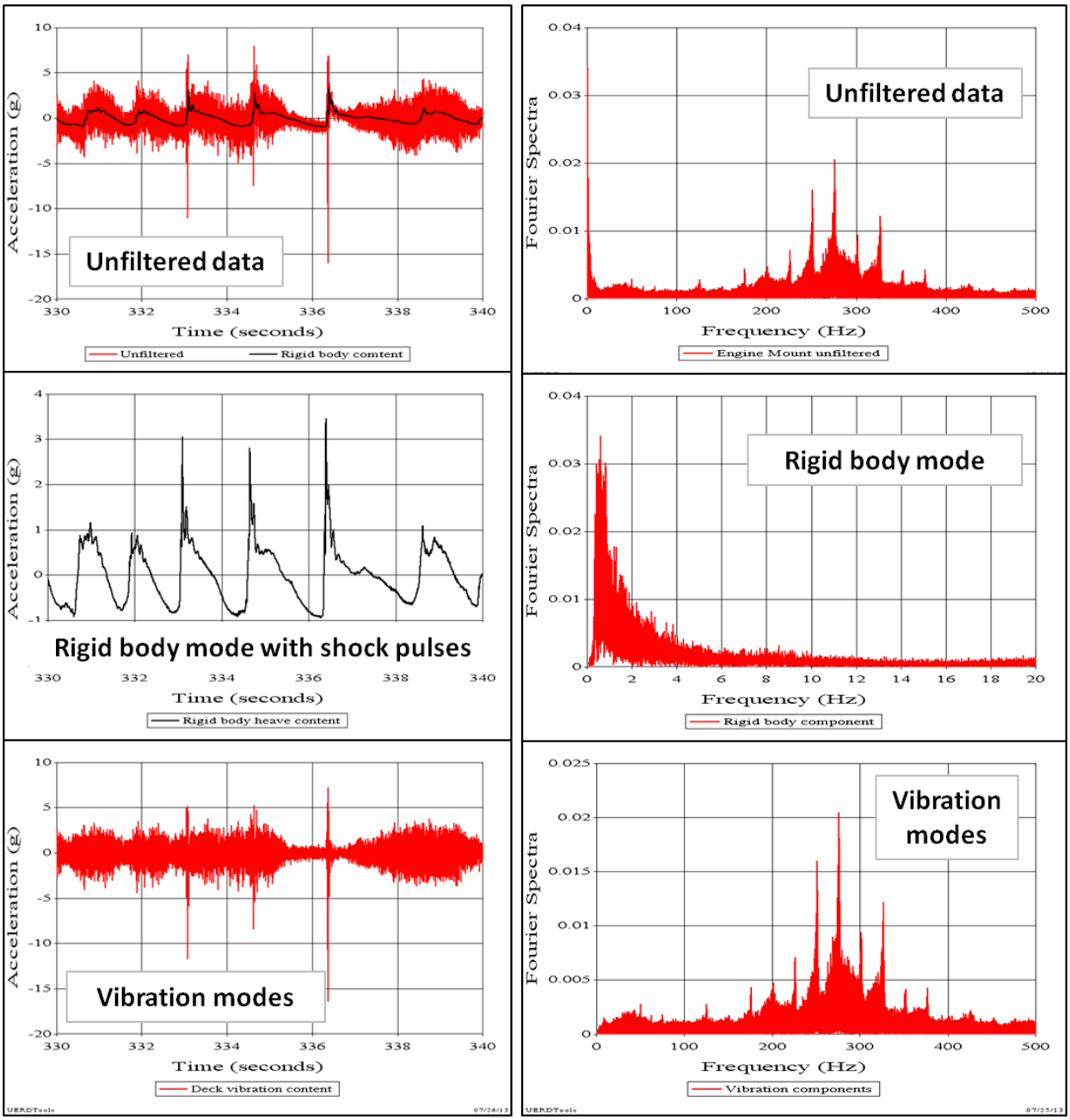

Figure 18. Modal Decomposition of Engine Mount Data

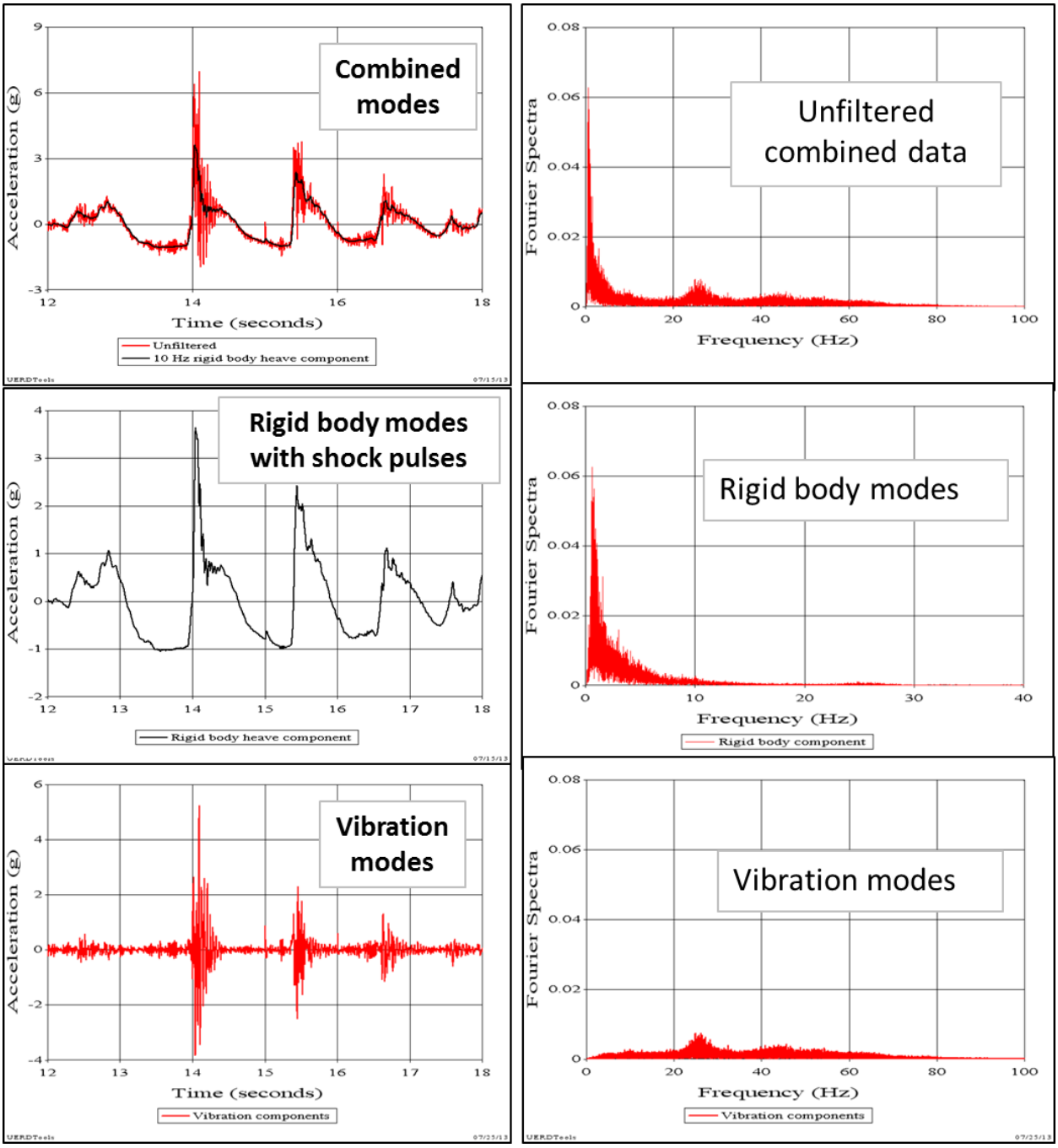

Figure 19. Modal Decomposition of Stiff-Deck Acceleration Data

Vibration Frequency and Displacements

As vibration frequency increases, the displacements of the oscillations decrease. This is true for steady state and forced transient vibrations. The velocity decreases with the inverse of the frequency, and the displacement decreases with the inverse of the frequency-squared. This can be illustrated by considering a simple undamped steady-state vibration with a displacement given by equation (1).

$$d(t) = d_m \sin 2\pi f t \qquad \text{Equation (1)}$$

In equation (1) the subscript "m" denotes the maximum displacement, "*t*" is time and "*f*" is the frequency of the oscillation. By taking the derivative of equation (1), it can be shown that the velocity of the vibration is given by equation (2).

$$v(t) = d_m 2\pi f \cos 2\pi f t \qquad \text{Equation (2)}$$

Likewise, the acceleration time history given by equation (3) is obtained by differentiating equation (2).

$$a(t) = -d_m (2\pi f)^2 \sin 2\pi f t \qquad \text{Equation (3)}$$

Substitution of equation (1) into equation (3) eliminates the time variable and results in the following equation for displacement amplitude (d) as a function of acceleration amplitude (a) and frequency. The minus sign has been dropped for convenience.

$$d = \left(\frac{a}{4\pi^2}\right)\left(\frac{1}{f^2}\right) \qquad \text{Equation (4)}$$

Equation (4) can be rewritten as equation (5) when the acceleration (a) is in units of g, the displacement (d) is in inches, and frequency (f) is in hertz.

$$d = 9.78a\left(\frac{1}{f^2}\right) \qquad \text{Equation (5)}$$

It can also be shown that the velocity of the oscillation is given by equation (6), where velocity (v) is in feet per second, acceleration (a) is in units of g, and frequency (f) is in hertz.

$$v = 5.11\,a\left(\frac{1}{f}\right) \qquad \text{Equation (6)}$$

Equations (5) and (6) were used to generate the curves shown graphically in Figure 20. The plots on the left are acceleration, velocity, and displacement for a pure sine wave with acceleration (a) equal to 4 g and a frequency of 2 Hz. The plots on the right are acceleration, velocity, and displacement for a pure sine wave with acceleration (a) equal to 4 g and a frequency of 20 Hz. A ten-fold increase in frequency from 2 Hz to 20 Hz results in a one-hundred-fold decrease in displacement from +/- 9.78 inches to +/- 0.0978 inches.

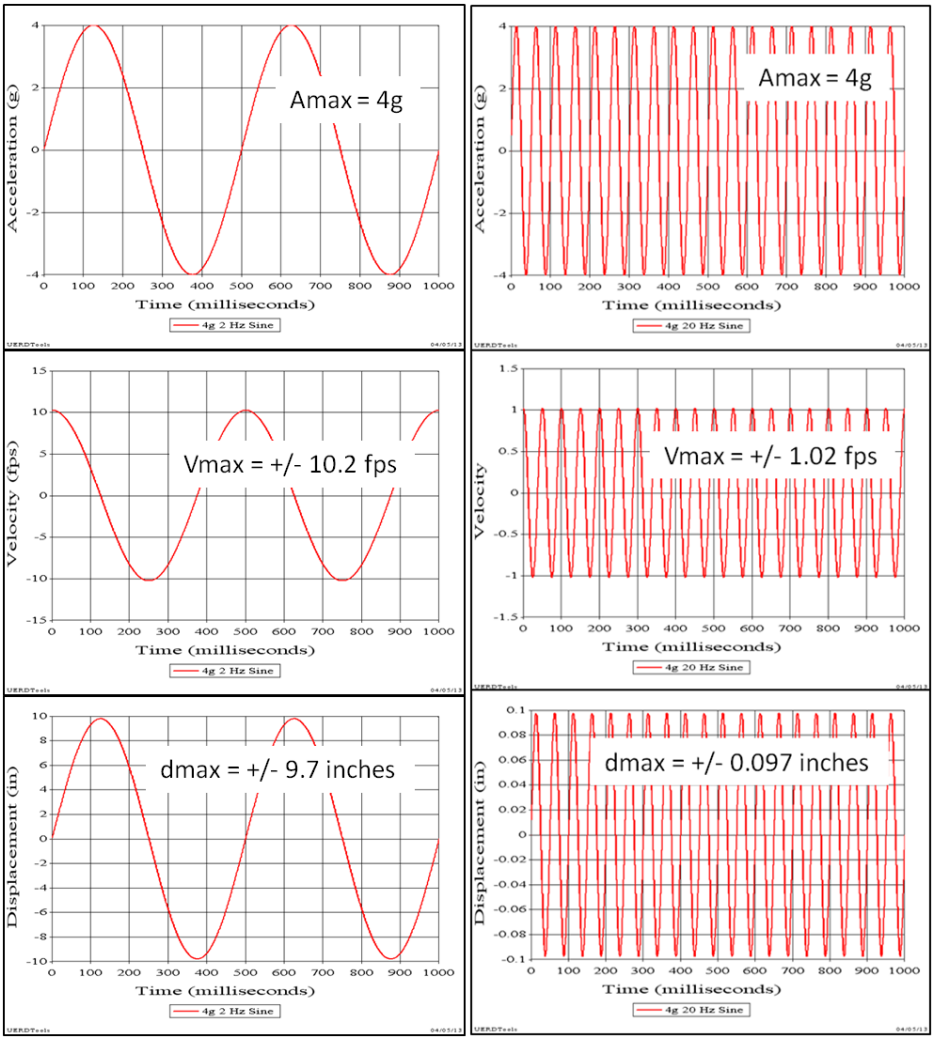

Figure 20. Pure Sine Wave Vibrations

Table 1 compares six different frequencies that all have the same 4 g maximum acceleration for a pure sine wave. For frequencies greater than 20 Hz the relative displacements computed by equation (5) rapidly approach thousandths of an inch. The table shows that vibrations on the order of 0.024 inches can have the same 4 g amplitude as displacements on the order of 9.7 inches to 39.1 inches (e.g., craft heave displacements). In the frequency domain, the magnitudes of acceleration spectra may be quite large, but the displacements associated with increasing frequency rapidly approach 1/100th to 1/1000th of an inch (e.g., 40 Hz to 80 Hz or

greater). Transient deck vibrations such as these transfer little or no load to system installations compared to the change in rigid body heave of a craft.

Table 1. Decreasing Vibration Displacements with Increasing Frequency

Frequency Hz	Acceleration g	Velocity fps	Displacement inches
1	4	20.440	39.120
2	4	10.220	9.780
10	4	2.044	0.391
20	4	1.022	0.098
40	4	0.511	0.024
80	4	0.256	0.006

The curves in Figure 20 and the tabulated displacements in Table 1 show how displacements decrease with increasing frequency for undamped sine-wave vibrations. In the real world of high-speed planing craft the deck displacements of damped forced-vibrations caused by wave impacts are also very small amplitude oscillations that can have large acceleration amplitudes. This is illustrated in Figures 21 and 22. Figure 21 shows the displacement time history of the vibration component obtained by double-integrating the engine mount vibration acceleration shown in the lower left of Figure 18. The vibration peak accelerations vary from +6 g to – 17 g with corresponding vibration displacements of +/- 0.044 inches or less.

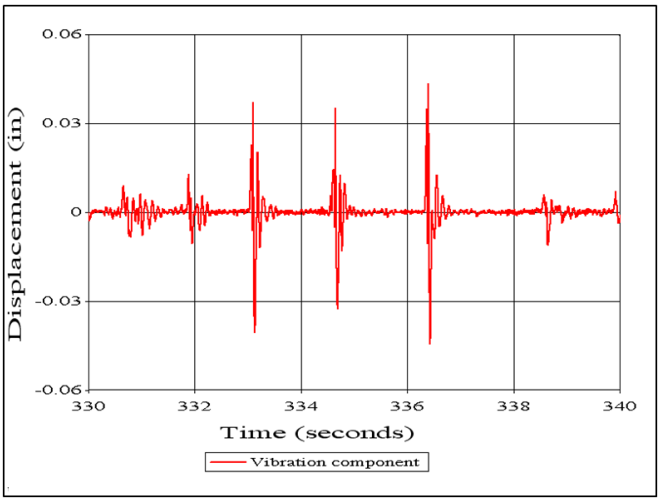

Figure 21. Engine Mount Vibration Displacement

Figure 22 shows the displacement time history of the vibration component obtained by double-integrating the stiff-deck vibration acceleration shown in the lower left of Figure 19. The vibration peak accelerations vary from + 5.2 g to – 3.8 g with corresponding vibration displacements of +/- 0.077 inches or less.

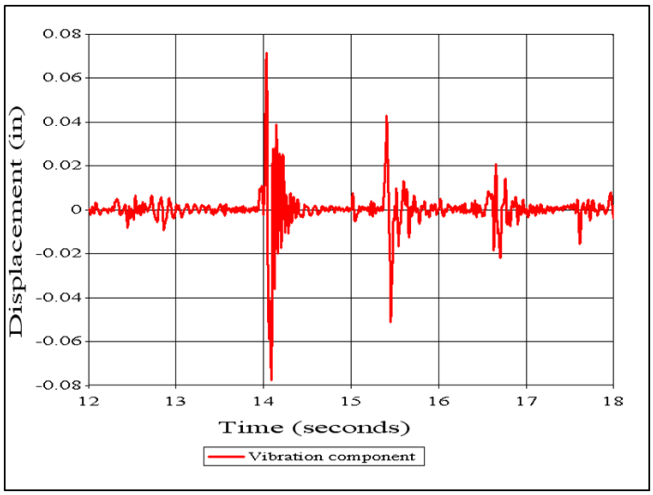

Figure 22. Stiff-deck Vibration Displacement

The magnitude of relative displacement responses is important because it helps to understand the characteristics of an acceleration signal with both rigid body heave and structural vibration content. This is especially important when acceleration data is being used to monitor load transmission from the keel up through a craft, and how the transmitted load affects hull structure, equipment, or personnel. The vibration acceleration content can have amplitudes equal to or greater than the rigid body content, but the vibration displacements will be very small and of little or no relative significance in transmitting wave impact load.

Observed Deck Response Frequency

Analyses of deck accelerometer data for 21 mono-hull planing craft less than 100 feet in length indicates that flexural responses are dominated by plate and stiffener vibrations in the vicinity of the gage. These response frequencies can vary on the order of 22 Hz to 85 Hz depending upon gage location and the surrounding support structure [12]. For these craft, analyses of Fourier spectra of recorded acceleration data indicated that a 10 Hz low-pass filter was appropriate to extract the rigid body accelerations from vertical and fore-aft acceleration data. The presence of a global hog-and-sag hull-girder flexural mode has not been observed for craft of this size (see Figure 13).

Quantifying Wave Impact Load

Acceleration Pulse Shape

The shape of the rigid body acceleration pulse during the impact time period can be simplified for analytical study as a half-sine pulse [12, 13]. This is illustrated by the eight example curves shown in Figure 23. The 10 Hz low-pass filtered data plots show the repeatable shape of rigid body acceleration responses when they are each normalized with respect to the peak acceleration in the record. The original peaks for each response varied from 1.9 g to 5.3 g.

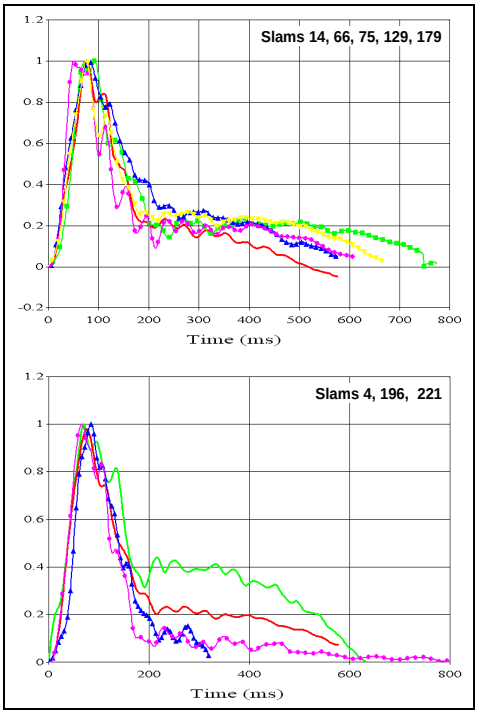

Figure 23. Half-sine Approximation of a Wave Slam Acceleration Pulse

The pulse durations vary from approximately 165 milliseconds to 220 milliseconds. The different colors represent different acceleration pulses for individual slam events. The slam numbers on each plot denote the time in seconds at which the impact occurred. The general observation is that the half-sine shapes of the acceleration pulses are approximately the same when impact forces dominate. While the sequence of wave encounters in terms of wave height and time between impacts is random, the vertical response of the craft to a single wave impact appears to be repeatable in shape with amplitudes that vary primarily with speed, craft weight, wave period, and wave height [2].

Acceleration Pulse Amplitude

The use of a half-sine acceleration pulse has been used extensively for establishing criteria for shock testing and impulsive load investigations [13 to 21]. Figure 24 illustrates the half-sine representation of a wave impact acceleration pulse where the largest amplitude is A_{peak} and the duration is T. Both the peak acceleration and the duration should be used to quantify the severity of the rigid body acceleration during a wave impact.

The area under the acceleration pulse in Figure 24 is the change in velocity caused by the wave impact. It is another very important parameter for characterizing the severity of a shock load. It can be shown that the change in velocity for the half-sine pulse is given by equation (7), where V is change in velocity in ft/sec, A_{peak} is the maximum acceleration amplitude in units of g, and T is the pulse duration in seconds.

$$V = \frac{64.4}{\pi} A_{peak} T \qquad \text{Equation (7)}$$

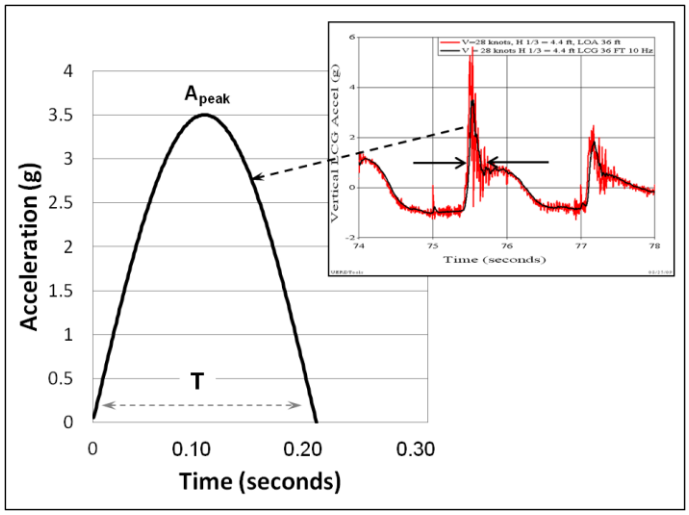

Figure 24. Half-sine Pulse Approximation of Wave Impact Acceleration Pulse

StandardG

StandardG is a software package that applies a four-step process to recorded acceleration data to extract the peak accelerations associated with the rigid body motions of planing craft. It was developed and refined by the Naval Surface Warfare Center, Carderock Division, Detachment Norfolk as an in-house tool to calculate craft acceleration statistics. Rigid body accelerations can then be used in reverse-engineering processes to estimate dynamic loads caused by wave impacts. The first two steps apply principles of response mode decomposition to determine rigid body content in the recorded acceleration signal. The second two steps were

developed specifically for computing unambiguous average of the highest $1/N^{th}$ peak accelerations used in naval architecture applications. The use of the *StandardG* four-step process enables comparisons of acceleration data results developed by independent researchers and among different organizations [22].

The *StandardG* algorithm for extracting rigid body peak accelerations from full-scale acceleration data and computing standardized $A_{1/N}$ values is available for evaluation from John Zseleczky, P.E., Branch Head, Hydromechanics Lab, U.S. Naval Academy, johnz@usna.edu, (410) 293-5102. It can be run by MATLAB™ or Octave™ software. The information package includes sample raw acceleration data, explanatory text files, computational results, and applicable papers and reports. The algorithm was specifically developed for computing rigid body $A_{1/N}$ accelerations [23] using acceleration data acquired using accepted instrumentation practices [24].

Figure 25 shows an example unfiltered acceleration record for a planing hull in head seas. The plot shows hundreds of wave impacts during the 528-second run. The plot shown in Figure 26 shows output from the *StandardG* algorithm for the acceleration record shown in Figure 25. The filtered (10 Hz low-pass) peak accelerations for each of the 344 wave impacts larger than the RMS value are plotted largest to smallest. The RMS acceleration was 0.64 g. The largest peak acceleration (labeled in the figure as A_{max}) was 4.63 g, $A_{1/100}$ was 4.19 g, and $A_{1/10}$ was 2.75 g.

The results shown in Figure 26 are applicable to one craft at one specific average speed for one significant wave height. The next section summarizes data trends that show how the peak acceleration amplitudes vary with craft weight, average speed, and significant wave height.

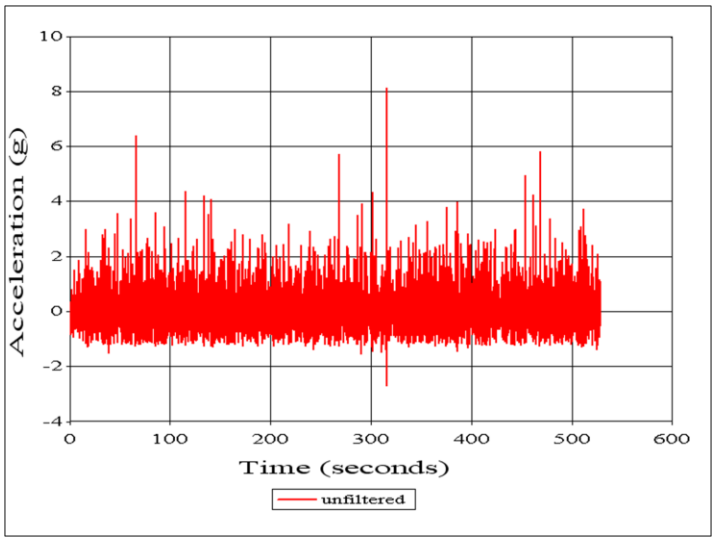

Figure 25. Example Unfiltered Acceleration Record

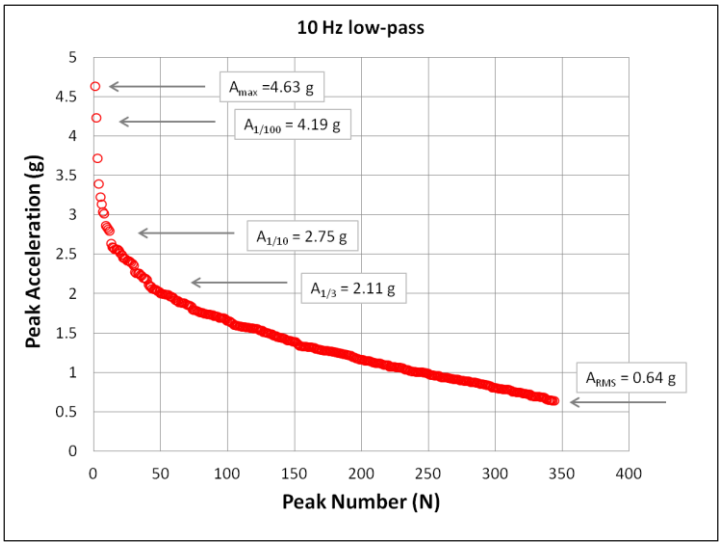

Figure 26. *StandardG* Algorithm Peak Acceleration Output

Peak Acceleration Trends

The following empirical equations for estimating acceleration pulse shape amplitude and duration where developed using $A_{1/100}$ and $A_{1/10}$ values calculated by the *StandardG* algorithm. They are based on a limited full-scale data base, but the observed trending results suggest they are useful for naval architecture and marine engineering applications until additional data is available. The shortest pulse duration for all peak accelerations greater than 2.0 g was on the order of 100 milliseconds. Identifiable trending results were observed only when data was parsed into two weight categories. Category A craft weighed from approximately 14,000 pounds to 18,000 pounds. Category B craft weighed from approximately 22,000 pounds to 38,000 pounds. They are based on trends in rigid body accelerations for manned and unmanned craft operating in head seas with short average wave periods (i.e., 3.4 to 6.4 seconds)[2] . Appendix A provides additional information on the range of database parameters and data correlation plots.

Equations for Category A Craft

The following equations apply to craft that weigh from 14,000 pounds to 18,000 pounds with lengths from 36 feet to 40 feet and beams from 8.5 feet to 9.0 feet. Testing conditions for this subset of data varied from roughly 21 knots to 45 knots with significant wave heights from approximately 2 feet to 4 feet. The equations estimate vertical accelerations in units of g at the longitudinal center of gravity (LCG) of the craft. V_s is craft average speed in knots, and $H_{1/3}$ is significant wave height in feet. T is the maximum duration of the half-sine acceleration pulse in milliseconds observed for a given value of A_{peak}. A_{peak} is the peak amplitude for a single wave impact.

$$A_{1/100} = \frac{(V_S + 12.63)(H_{1/3} - 0.73) - 11.14}{21.72} \qquad \text{Equation (8)}$$

[2] Limited distribution report NSWCCD-23-TM-2012/38, October 2012.

$$A_{1/10} = \frac{(V_S + 0.77)(H_{1/3} - 0.70) - 5.52}{25.6} \quad \text{Equation (9)}$$

$$T = 287 - 27.7\,A_{peak} \quad \text{Equation (10)}$$

Equations for Category B Craft

The following equations apply to planing craft that weigh from 22,000 pounds to 38,000 pounds with lengths from 33 feet to 48.9 feet and beams from 9 feet to 15 feet. The craft in Category B were tested in seas with significant wave heights ranging from 2.4 feet to 5.7 feet with average speeds from 10.0 knots to 39.6 knots. The equations estimate vertical accelerations in units of g at the longitudinal center of gravity (LCG) of the craft. V_s is craft average speed in knots, and $H_{1/3}$ is significant wave height in feet. T is the maximum duration of the half-sine acceleration pulse in milliseconds observed for A_{peak} greater than 2.0 g. A_{peak} is the peak amplitude for a single wave impact.

$$A_{1/100} = \frac{(V_S + 21)(H_{1/3} - 1.03)}{56.83} - 0.20 \quad \text{Equation (11)}$$

$$A_{1/10} = \frac{(V_S + 7.46)(H_{1/3} - 1.08)}{62.5} \quad \text{Equation (12)}$$

$$T = 433 - 55\,A_{peak} \quad \text{Equation (13)}$$

Impact Velocity

Interest in the velocity parameter is not new. The original theory developed in 1929 for predicting the maximum pressure acting on seaplane floats during water impact focused on the velocity at the moment of first contact [25]. Subsequent experimental investigations that used drop testing with solid wedges impacting a water surface applied this theory and demonstrated that the velocity parameter correlated well with the pressure during a wave slam [26]. It combines the acceleration amplitude and the duration parameters, so it is an important parameter for investigating the damage potential of dynamic loads [27 to 29]. The change in velocity is a critical parameter for specifying laboratory drop tests that simulate the effects of severe impacts [30, 31].

There are two approaches for estimating the change in vertical velocity recorded during wave impacts for planing craft[3]. The first approach is to apply direct integration to recorded acceleration records to obtain impact velocities for each wave impact. The second approach is to use equation (7) for a given peak acceleration and pulse duration time.

The first approach is illustrated by Figures 27 and 28. Figure 27 is a 20-second segment of the acceleration record in Figure 25 that shows 14 wave impacts. This record was subjected to a 0.025 Hz high-pass filter to remove or minimize drift in the integration process. Figure 28 shows the velocity plot obtained by integrating the acceleration in Figure 27. In this record the change in velocity due to each of the 14 wave impacts is the absolute value of the largest negative velocity before each impact.

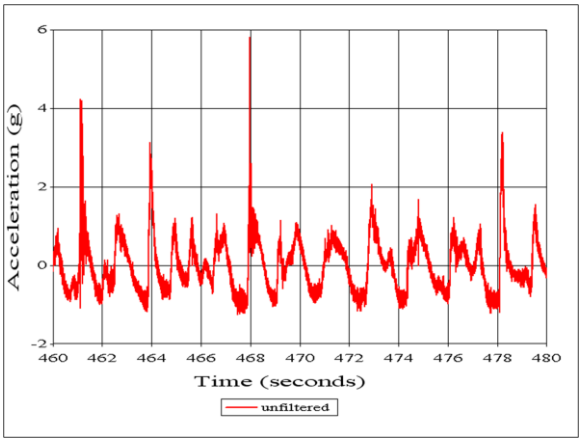

Figure 27. High-pass Filtered 0.025 Hz Acceleration

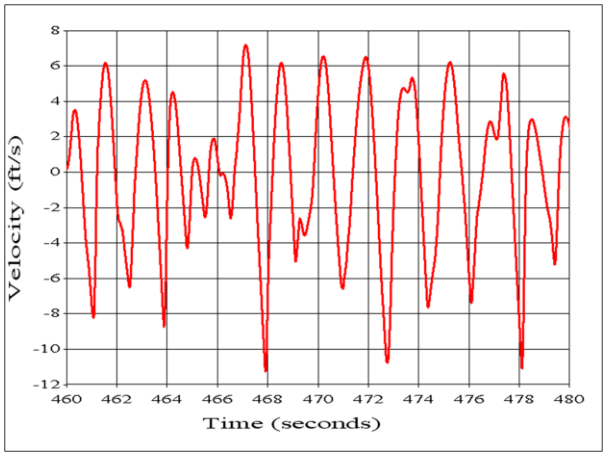

Figure 28. Velocity from Integration of Acceleration Record

Appendix B shows that for the data analyzed a 0.025 Hz high-pass filter applied to the acceleration record prior to integration effectively minimizes velocity drift without significantly

[3] Limited distribution report NSWCCD-TM-2012/36, September 2012.

affecting the velocity peak amplitudes. Appendix B provides additional discussions on high-pass filtering effects.

An effective approach to determining the impact velocity for all wave impacts in a record includes the following steps.

1. Multiply the velocity time history (like the segment shown in Figure 28) by negative one to invert the record.

2. Input the inverted record into the *StandardG* algorithm to extract only the peak velocity values. This approach is appropriate because *StandardG* is not just an acceleration algorithm. It is a general purpose code for peak amplitude extraction tailored to wave impact sequences. It is recommended that the RMS velocity be used as the vertical threshold in the *StandardG* velocity computation.

An example of the results of this process is shown in Figure 29. The algorithm identified 277 peak velocities greater than the root-mean-square velocity (which was 4.22 fps). The largest impact velocity was 15.93 fps. The average of the highest one percent, ten percent, and 33.3 percent are also shown. Appendix B provides additional discussions related to this process.

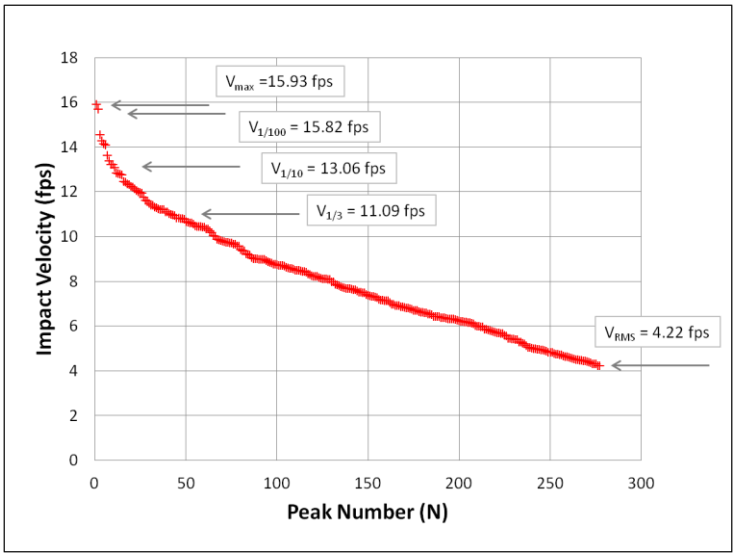

Figure 29. Sorted Peak Velocities Plotted Largest to Smallest

The Effects of Wave Impacts

Loading Complexity

The investigation of the effects of wave impacts on craft systems will be presented in three topic areas of interest. The first area of interest is the hull structure and methods used in design for impact loads. The second topic area of interest is the ability of shock mitigation seats and mechanical and electrical systems to perform their functions under impulsive loads. The third area of interest is human comfort and performance in rough seas. Another topic area of interest dealing with the potential for human injury could be considered, but it is beyond the scope of this report.

Investigation of the effects of wave impacts for each of the three topic areas can be approached from two perspectives. The first involves the study of the effects of a single impulsive load on a system. The second perspective involves investigations into the cumulative effects of multiple impact loads over time, as in the effects of material fatigue. Figure 30 illustrates these two approaches. The category of multiple impacts can be further sub-divided into multiple impacts with constant severity and multiple impacts of changing severity. The figure shows a third element aspect of the taxonomy that addresses different levels of complexity for the topic areas under investigation. The complexity level deals with the nature of the loading, and whether it is a single impulse (Level I), or repeated impulses of constant severity (Level II), or repeated impulses with changing severity (Level III).

The increasing complexity levels in Figure 30 are meant to be a reflection of the increasing number of variables when studying the three topic areas of interest. In Level I the focus is on the effect of one impact on a system. It was shown in an earlier section of this report that this level of study is important because in planing craft the system time history responses to one wave impact damp out before the next wave impact. This means that each wave impact can be studied and analyzed as a single event. In Level II the investigation adds the cumulative effects over time of multiple impacts of constant severity. Level II with a constant wave impact severity is referred to as a regular sea condition. In Level III the investigation adds further complexity in the variability of the severity of the impulses over time. Level III is referred to as an irregular sea conditions (i.e., variable impacts over time as a function of sea conditions). This taxonomy suggests that a full knowledge of cause and effect relationships in Level I is a prerequisite for study in Levels II and III. Level I and Level II investigations may be of interest for design applications where the designer may be interested only in the maximum anticipated load conditions (e.g., study of structure or equipment ruggedness). Level III investigations add the complexity and statistics of random ocean waves over time (e.g., human comfort and performance).

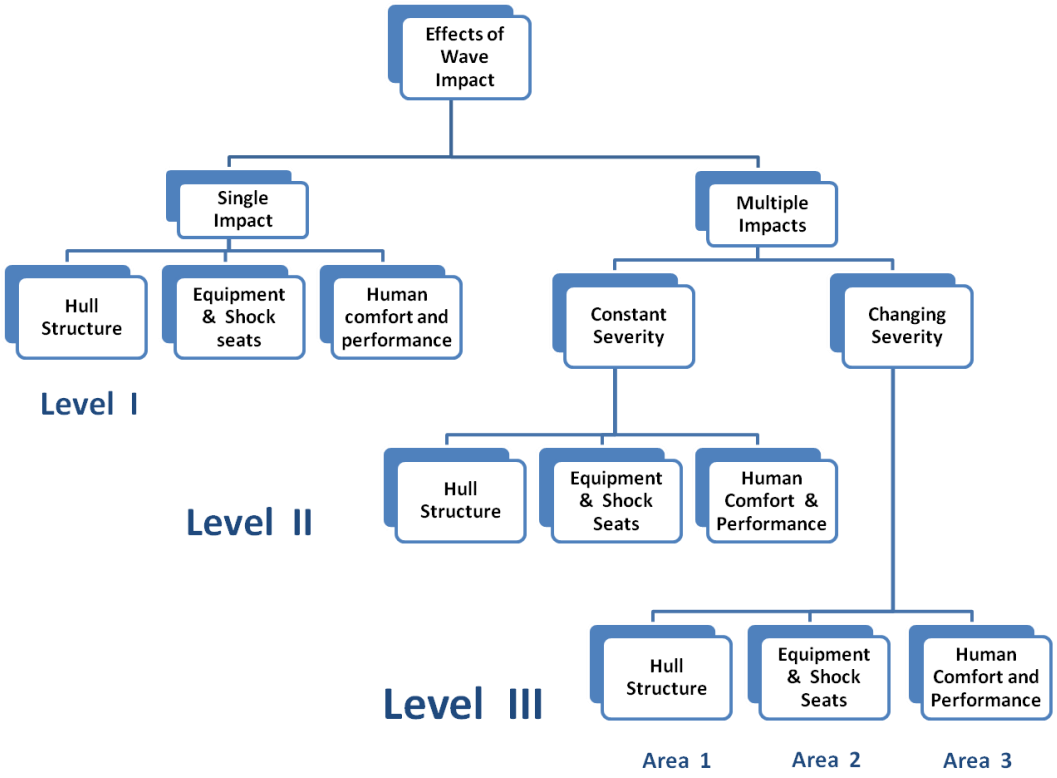

Figure 30. Complexity of Wave Impact Investigations

Hull Structure Application

The design of hull structural elements for high-speed planing craft is based on an approach originally published in 1978 that computes an equivalent static pressure associated with the dynamic pressure acting on the hull bottom during wave impacts [32]. It is computed by multiplying an acceleration value (referred to originally as the impact load factor) by parameters that account for the displacement of the craft and the area over which the impact load acts. It was reported that the most controversial part of the design process involved the source of the acceleration value to be used in the equations.

A recent application of modal decomposition of acceleration data described in this report provides a physics-based rationale for computing an equivalent static acceleration to be used in hull structure design equations [12]. Figure 31 shows an example plot of peak accelerations recorded during 151 wave impacts. They are rigid body peak accelerations obtained from an acceleration time history by using the *StandardG* algorithm. The peak acceleration of the most severe wave impact (i.e., A_{max}) is 5.31 g.

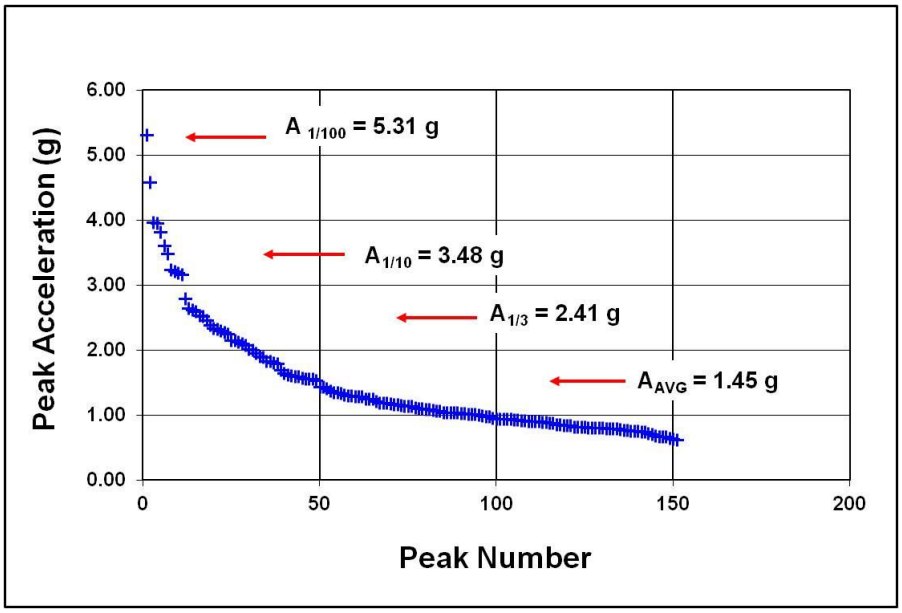

Figure 31. Rigid Body Peak Accelerations Plotted Largest to Smallest

If it is assumed that the data was recorded in an environment that corresponds to the maximum design speed for the craft and the maximum operational significant wave height (with an average wave period less than roughly 6.5 seconds), then the most severe load for hull design can be characterized by a rigid body half-sine pulse with a maximum amplitude of 5.31 g and a duration T. It can be shown that the equivalent static acceleration for hull design for a half-sine acceleration pulse is given by equation (14) [12].

$$Equivalent\ Static\ Acceleration\ (ESG) = \frac{2}{\pi} A_{\max} \qquad \text{Equation (14)}$$

The equivalent static acceleration of 5.31 g shown in Figure 31 is 3.38 g. The ESG value is a convenient parameter that enables investigations of the static strength of materials for structures operating in dynamic environments. The use of the ESG for investigating craft structural strength could also be extended into a Level II investigations by considering the effects of constant impact loads over time (i.e., as in material fatigue investigations).

Equipment Ruggedness

When high-speed craft encounter very rough seas the typical reaction by experienced operators is to slow down. This action significantly reduces the severity of the wave impacts. But during full-scale trials intended to push the craft to its limits, or during military operations, or during competitive racing events the operators may not slow down, and the more severe wave impacts can lead to equipment malfunction or failure.

A recent study that applied the rigid body equations described in this report led to the development of a laboratory drop test procedure that could be used to test equipment items prior

to craft installation to ensure they were sufficiently rugged to withstand severe and repeated wave impacts [21]. The wave impact velocity given by equation (1) can be converted to an equivalent drop height using equation (15), where the velocity V is in fps, g is 32.2 ft/sec^2, and the drop height H is in feet.

$$H = \frac{V^2}{2g} \qquad \text{Equation (15)}$$

For example, the impact velocity values shown in Figure 29 can be converted to the equivalent drop heights shown in Figure 32. The drop height for the largest impact velocity (15.93 fps) is 3.9 feet.

In order to simulate the vertical rigid body acceleration of a wave impact, the falling equipment item must experience an acceleration pulse upon impact with a shape that simulates the vertical half-sine acceleration pulse shown in Figure 24. This is typically achieved at drop test facilities by placing a pliable object or energy absorbing device on the impact surface that achieves the proper duration and shape of the load deceleration pulse.

As an example, equations (7), (10), and (15) can be used with the largest peak acceleration shown in Figure 31 (i.e., 5.31 g) to generate a drop test scenario for equipment for Category A craft. Equation (10) yields a pulse duration of approximately 0.14 seconds. Equation (7) yields a velocity of 15.2 fps, and the equivalent drop from equation (15) is 3.6 feet. The drop test would be from a height of 3.6 feet onto a pliable surface that results in a roughly half-sine pulse upon impact with amplitude of 5.3 g and 0.14-second duration.

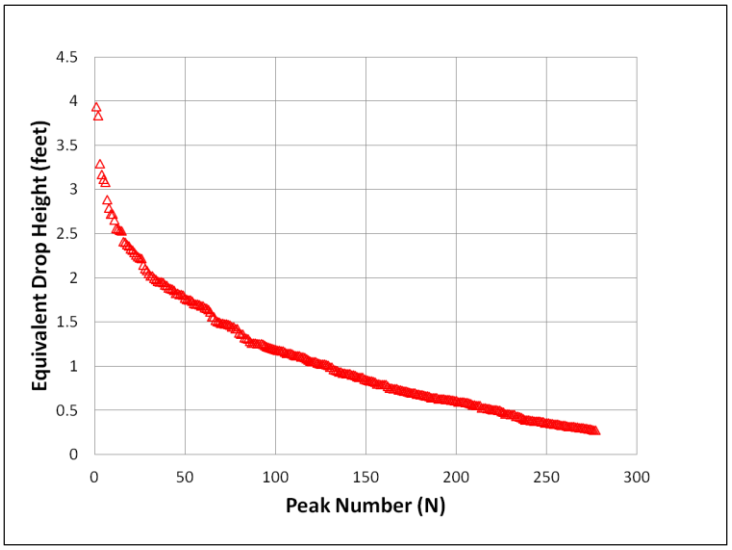

Figure 32. Equivalent Drop Test Heights for Wave Impacts Sorted Largest to Smallest

The use of vertical acceleration data (i.e., rigid body A_{max} and T) to develop the drop test protocol is based on the assumption that the major damage mechanisms in equipment

components are associated with vertical forces (i.e., compressive forces). For cases where fore-aft or port-starboard accelerations could also lead to damage potential, half-sine representations of those accelerations could also be used to tailor a more complex drop test. For example the vertical drop test apparatus could include a test fixture that rotates the test item by some angle to achieve multi-axis acceleration inputs.

Another consideration for equipment ruggedness in planing craft is the potential for equipment malfunction or failure to occur after repeated low amplitude impacts over a long period of time (i.e., a Level II investigation in Figure 30). For example, sensitive electronic systems must be sufficiently rugged to withstand wave impacts. One approach to demonstrating equipment operability over long periods of time is to subject the equipment to laboratory testing with constant lower severity impulses [21]. The amplitudes of the repeated impulses would be less than the A_{max} acceleration amplitude used in the equipment drop test. For example, cyclic low-amplitude impact testing could be performed on a shaker table or an impact machine in a laboratory.

Evaluation of Shock Mitigation Seats

The same drop test procedure described above for equipment can also be used for demonstrating in a laboratory environment the level of mitigation achieved by shock mitigation seats or deck mats installed as energy absorbing material [33].

Human Comfort and Performance

In the absence of recent experimental data on human performance, the following discussion is presented to show how the unified approach of using rigid body accelerations values can be used with performance criteria.

Human comfort and performance criteria were reported in the 1970's and 1980's based on feedback from naval crews immediately following rough-water seakeeping trials[4] [5]. It was reported that the severity of vertical accelerations in a planing craft characterized by $A_{1/10}$ less than 1.0 g (rigid body) corresponded to an environment where the crew could effectively perform their functions for 4 or more hours. A value of $A_{1/10}$ equal to 1.5 g (rigid body) corresponded to the crew being able to perform effectively for 1 to 2 hours exposure. Other values listed in Table 2 were subsequently published [34, 35], but it was known that they were not to be interpreted as fixed values that apply equally to all individuals. People can exhibit large variation in response to the environment, and the tolerance of one person may not be consistent [36, 37]. For example, hypothetically, one individual may experience 1 to 2 hour limited performance after being exposed to $A_{1/10}$ equal to 1.3 g while another individual may experience the same effects at 1.7 g.

[4] Limited distribution report DTNSRDC-SDD-114-24, August 1976.
[5] Limited distribution report NAVSEACOMSYSENGSTANORVA 60-115, August 1983.

Table 2. $A_{1/10}$ Acceleration Criteria for Personnel Effects

A 1/10 (g) at LCG	Effects on Personnel
1.0	Maximum for millitary function long term (over 4 hours)
1.5	Maximum for military function short term (1 - 2 hours)
2.0	Tests discontinued
3.0	Extreme discomfort
4.0	-
5.0	Physical injury
6.0	Military crew under fire

Rigid body $A_{1/10}$ values listed in Table 2 were converted to ranges of values based on observed variations in acceleration data that align with the concept of human variability [38]. These ranges are shown in Table 3.

Table 3. Crew Comfort and Performance Transition Zones

Severity Transition Zones	A 1/10 (g)	A 1/10 Range (g)	Condition
IV	3	3g - 4g	Extreme Discomfort
III	na	2 g - 3 g	Discomfort and limited mission performance
II	1.5	1 g - 2 g	Effective mission performance for 1 - 2 hours
I	1	<1 g	Effective mission performance for 4 or more hours

The values listed in Table 3 can be used with equation (9) or equation (12) to plot zones that show regions where performance limitations or discomfort might be expected. Figure 33 shows an example crew comfort and performance plot for Category B craft.

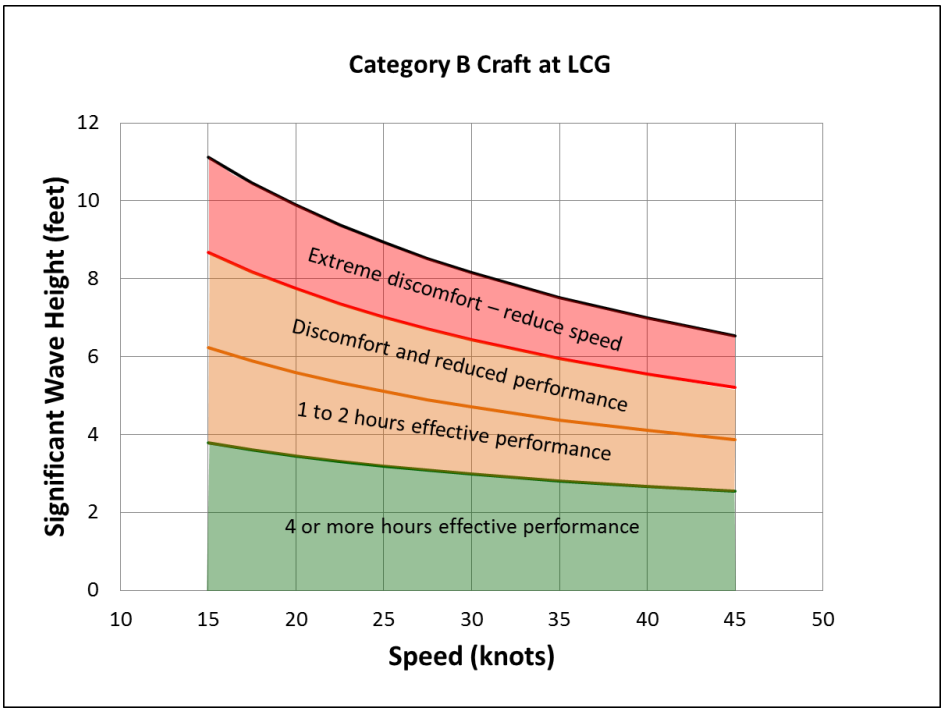

Figure 33. Speed vs. Wave Height Envelopes for 22K – 38K Pound Craft

The use of the $A_{1/10}$ parameter to construct Figure 33 is not unique. The same curves could also have been constructed using the $A_{1/100}$ equations presented in this report [38]. The use of the $A_{1/100}$ parameter requires that the values listed in Tables 2 and 3 be converted from $A_{1/10}$ to $A_{1/100}$ using available experimental data. What is unique in this example is the use of a statistical acceleration value (i.e., $A_{1/10}$ or $A_{1/100}$) to quantify a "load severity" that varies over time. The use of a statistical acceleration value is therefore aligned with Level III investigations that study the effects of random wave impacts over time.

Consistent Modeling Approach

The four example applications of investigating the effects of planing-craft wave impacts illustrate the three levels of investigation complexity shown in Figure 30. Level I considered the effect of a single severe impact on structure and equipment. Level II considered the effects of material fatigue on a structure or the effects over time of repeated low severity impacts on sensitive electronics equipment. Level III considered the effects over time of a varying impact severity on human comfort and performance by using a statistical acceleration parameter (i.e., $A_{1/N}$). The common denominators among all three are (1) the consistent use of an assumed pulse shape to model the impulsive load, and (2) the consistent use of a load severity parameter (i.e., rigid body heave acceleration) obtained from trials data using an acceleration response mode decomposition process. This consistent modeling approach provides a unified approach to analyzing the response of any system at a cross section on a planing craft with the same mathematical representation of a wave impact load.

Scale Model Application

Use of a low-pass filter to remove vibration content in an acceleration record has also been reported for data obtained during scale-model testing in a tow tank [3]. The displacement of the planing hull model was approximately 14.33 pounds. It had a waterline length of approximately 37.4 inches and a beam of approximately 9.8 inches. Figure 34 is a figure from reference 3 that shows the rigid body portion of a vertical acceleration signal (green curve) obtained from low-pass filtering, and the vibration component (black curve) extracted using a high-pass filter. The rigid body acceleration was used to compute the inertia force of the wave impact which was then compared with recorded pressure data (i.e., cited earlier in this report).

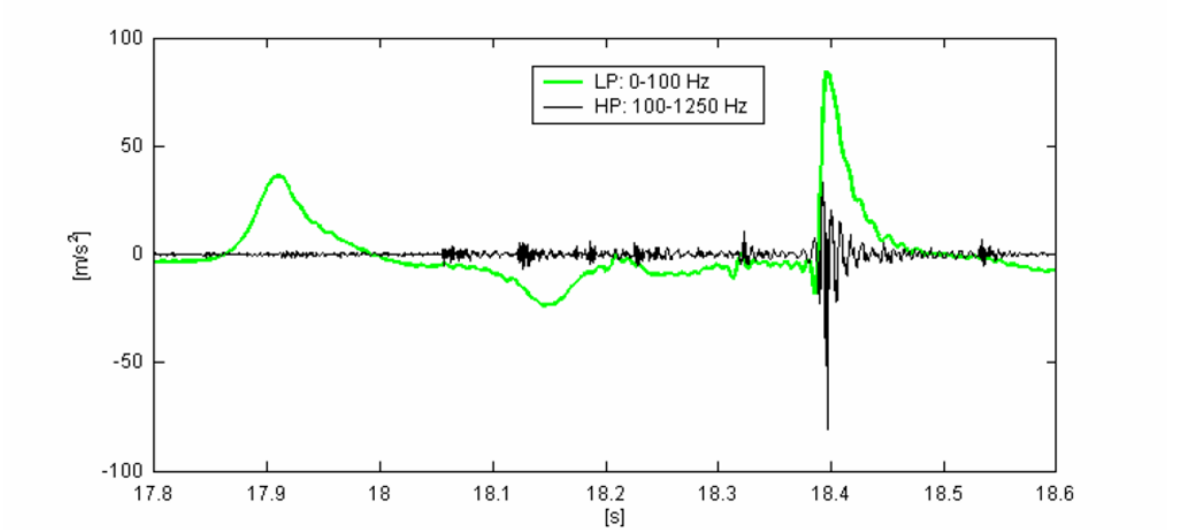

Fig. 7. Example of the accelerometer signal at the bow (A_2). The low-pass part of the signal (LP) is assumed to represent the rigid body acceleration and the high-pass part (HP) is concluded to be structural vibrations.

Figure 34. Rigid Body and Vibration Components in Scale-Model Data

It is important to note that the amplitude of the low-pass filter used to extract rigid body acceleration will depend upon time-scaling considerations. Therefore, the appropriate low pass filter will vary from full scale to model scale and from one model scale to another. Analyses of the full-scale data referenced in this report led to the use of a 10 Hz low-pass filter to estimate rigid body peak accelerations on full-scale. The choice of the cut-off level is an important issue [3] on full-scale and model-scale, so additional research is recommended to investigate how vibrations can be effectively removed without loss of important physical information.

Conclusions and Recommendations

Accelerometers are very sensitive instruments that measure flexural motions of deck plates and stiffeners as well as rigid body motions like heave, surge, pitch, and roll and structural vibrations. The recorded acceleration is therefore a superposition of different response modes that depend upon the location of the gage.

An unfiltered acceleration record should initially be labeled in units of length per time-squared because it is a recording of the rate of change of velocity at the location of the gage. If data plots of unfiltered acceleration time histories are normalized by dividing by the acceleration due to gravity they should not be labeled “g-load”.

Analyses of an unfiltered acceleration time history and its Fourier spectrum can be used to decompose the unfiltered record in the frequency domain into its different modes of response. The process of decomposing an acceleration record into its different modes of response is referred to as response mode decomposition. The modes of response include rigid body modes (e.g., heave, surge, pitch, roll, etc.), local deck and stiffener flexural modes (i.e., local response vibrations), response modes of isolated equipment or shock mitigation seats, and, if the craft is large enough, global hull-girder flexure.

The rigid body acceleration response can be decomposed from an unfiltered acceleration record by using a low-pass filter. For small high-speed planing craft less than 100 feet in length it is recommended that a 10 Hz low-pass filter be used to enable broad correlations and comparisons, unless Fourier spectra analyses indicate that some other filter frequency should be used. If a different amplitude is used it should be published with the analysis results.

In the absence of a practical hull force gage or pressure gage, the impulsive load of a wave impact can be quantified by the amplitude and duration of the rigid body acceleration response during the impact. This relationship exists because the response periods of structural vibrations in craft are less than the typical 100 msec (or more) duration of wave impacts.

It is recommended that the vertical acceleration pulse used to characterize the wave impact load for high-speed planing craft be mathematically modeled as a half-sine pulse. The area under the wave impact half-sine pulse is the change in heave velocity caused by the impact. It is a useful parameter for quantifying impact severity. For constant mass it is a direct measure of the change in momentum caused by the impulsive load. Another useful parameter for quantifying the severity of a wave impact load is the equivalent drop test height. It is determined by substituting the wave impact velocity into equation (15).

It is recommended that integration of acceleration records to obtain wave impact velocities be performed only after the acceleration record is demeaned (i.e., recorded average acceleration equal to zero) and initially subjected to a 0.025 Hz high-pass filter, unless the Fourier spectrum indicates another filter frequency should be used. High-pass filtering the signal avoids or

minimizes drift caused by the integration process without significantly decreasing the velocity peaks.

The response of any system onboard a craft should be able to be evaluated with the same mathematical representation of a wave impact load. This is true regardless of whether it is related to hull structural strength, the ruggedness of sensitive onboard equipment systems, the response of shock mitigation seats, or studies of human comfort and performance. It is recommended that the methods presented in this report be used as a consistent approach for quantifying the effects of wave impact loads on high-speed planing craft.

Symbols, Abbreviations, and Acronyms

α ..... impact angle of deck relative to horizon
A_{peak} or A_{max} ..... peak or maximum vertical acceleration
b ..... craft beam
c ..... critical damping coefficient
deg ..... degrees
f ..... system natural frequency
ft ..... feet
fps ..... feet per second
g ..... acceleration due to gravity (32.2 ft/sec^2)
$H_{1/3}$ ..... average of the 1/3rd highest wave heights, significant wave height
Hz ..... Hertz (cycles per second)
k ..... structural stiffness
kn ..... knot
L ..... length
LCG ..... longitudinal center of gravity
m ..... mass
msec or ms ..... millisecond
π ..... ratio of circle circumference to its diameter
sec ..... second
SDOF ..... single degree-of-freedom
T ..... wave impact shock pulse duration
V or V_v ..... vertical change in craft rigid body velocity
V_K ..... craft average speed in knots

References

1. Jacobson, A., Coats, T., Haupt, K., Pogorzelski, D., Jacobson, D, "Working Towards Vertical Acceleration Data Standards," Maritime Systems and Technology (MAST) Contone Congressi, Porto Antico, Genoa, Italy, 14 – 16 November 2007.
2. Riley, M., Coats, T., Haupt, K., Jacobson, D., "The Characterization of Individual Wave Slam Acceleration Responses for High-Speed Craft," Proceedings of the American Towing Tank Conference, Annapolis, Maryland, August 2010.
3. Rosen, A., and Garme, K., "Model Experiment Addressing the Impact Pressure Distribution on Planing Craft in Waves," Royal Institute of Naval Architects, International Journal of Small Craft Technology, Transactions Volume 146 Part B1, 2004.
4. Garme, Karl, Rosen, Anders, and Kuttenkeuler, Jakob, "In Detail Investigation of Planing Pressure," Proceedings of the HYDRALAB III Joint User Meeting, Hannover, Germany, February, 2010.
5. Harris, Cyril M., "Shock and Vibration Handbook Fourth Edition," McGraw Hill, New York, Chicago, San Francisco, 1996
6. Savitsky, Daniel and Brown, P.W., "Procedures for Hydrodynamic Evaluation of Planing Hulls in Smooth and Rough Water," Marine Technology, Volume 13, No. 4, October 1976.
7. Coats, Dr. Timothy, "Shock Mitigation – A Familiar Topic in High-Speed Planing Boat Design," 74th Shock and Vibration Symposium, 27 – 31 October, 2003, San Diego, California.
8. Riley, M. R., Coats, T.W., "A Simplified Approach for Analyzing Accelerations Induced by Wave Impacts in High-Speed Planning Craft," The Third Chesapeake Powerboat Symposium, Annapolis, Maryland, USA, 14-15 June 2012.
9. Riley, Michael R., Coats, Timothy, Dr., Haupt, Kelly, Jacobson, Donald, "Ride Severity Index: A Simplified Approach for Comparing Peak Acceleration Responses of High-Speed Craft," SNAME Journal of Ship Production and Design, Vol. 29, No.1, February 2013.
10. Jasper, N. H., "Dynamic Loading of a Motor Torpedo Boat (YP 110) During High Speed Operation in Rough Water," David Taylor Model Basin Report C-175, September 1949.
11. Blount, D., Hankley, D., "Full Scale Trials and Analysis of High Performance Planing Craft Data," Society of Naval and Marine Engineers Number 8, November 1976.

12. Riley, M. R., Coats, T.W., "Development of a Method for Computing Wave Impact Equivalent Static Accelerations for Use in Planing Craft Hull Design," The Third Chesapeake Powerboat Symposium, Annapolis, Maryland, USA, June 2012.

13. Gollwitzer, Richard M., Peterson, Ronald S., "Repeated Water Entry Shocks on High-Speed Planing Boats" Naval Surface Warfare Center Panama City Dahlgren Division Report CSS/TR-96/27, September 1995.

14. Buxbaum, Peter, "Easing the Ride: How Much Can You Mitigate Shocks on the Water," U.S. Coast Guard Forum Volume 2 Issue 2, KMI Media Group, May 2010.

15. Clough, Ray, W., Penzien, Joseph, "Dynamics of Structures," McGraw-Hill Book Company, New York, New York, 1975.

16. "Standard Test Method for Simulated Drop of Loaded Containers by Shock Machines," American Society of Testing and Materials (ASTM) Standard D5487, April 2008.

17. Department of Defense Test Method Standard, "Environmental Engineering Considerations and Laboratory Tests," Military Standard, MIL-S-810G, Method 516.6, Shock, 31 October 2008.

18. Department of Defense Test Method Standard, "Environmental Engineering Considerations and Laboratory Tests," Military Standard, MIL-STD-810G, Part One, Annex D, 31 October 2008.

19. Department of Defense Test Method Standard, "Electronic and Electrical Component Parts," Military Standard, MIL-STD-202G, method 213B, Shock, 16 April 1973.

20. Vierck, Robert K., "Vibration Analysis," International Textbook Company, Scranton, PA., 1967.

21. Riley, M.R., Haupt, K.D, Murphy, H.P., "Test Specification Guide for Electrical and Electronic Equipment to Withstand Wave Impacts in Planing Craft," Naval Surface Warfare Center Report NSWCCD-TM-23-2012/03, January 2012.

22. Riley, Michael R., Haupt, Kelly D., Jacobson, Donald R., "A Generalized Approach and Interim Criteria for Computing $A_{1/N}$ Accelerations Using Full-Scale High-Speed Craft Trials Data," Naval Surface Warfare Center Carderock Division Report NSWCCD-TM-23-2010/13, April 2010.

23. Zseleczky, John and McKee, Glen, "Analysis Methods for Evaluating Motions and Accelerations of Planing Boats in Waves," Hydrodynamics Laboratory, US Naval Academy, Davidson Laboratory, Stevens Institute of Technology, August 1989.

24. Zseleczky, John, "Behind the Scenes of Peak Acceleration Measurements," The Third Chesapeake Powerboat Symposium, Annapolis, Maryland, USA, 14-15 June 2012.

25. Von Karman, Th., "The Impact of Seaplane Floats During Landing," National Advisory Committee for Aeronautics Technical Note No. 321, October 1929.

26. Chaung, Sheng-Lun, "Slamming Tests of Three Dimensional Models in Calm Water and Waves," Report 4095, Naval Ship Research and Development Center, Carderock, MD, USA, September 1973.

27. Wolk, H., Tauber, J.F., "Man's Performance Degradation During Simulated Small Boat Slamming," Naval Ship Research and Development Center Report 4234, January 1974.

28. Heimenz, Gregory, Dr., "Adaptive Magnetorheological (MR) Shock Absorbers for High Speed Craft," Multi-Agency Craft Conference, 14 June 2011, Virginia Beach, Virginia.

29. "Standard Test Methods for Mechanical-Shock Fragility of Products, Using Shock Machines," American Society of Testing and Materials (ASTM) Standard D3332-99, January 2010.

30. Lang, G. F., "Why Do Things Break When We Drop Them," Sound and Vibration, pp. 12 – 13, April 2010.

31. Lang, B.W., "A New American National Standard for Shock Testing Equipment," pp. 13 – 14, Sound and Vibration, April 2010.

32. Allen, R.G. and Jones, R.R., "A Simplified Method for Determining Structural Design-Limit Pressures for High Performance Craft," American Institute of Aeronautics and Astronautics, Society of Naval and Marine Engineers Advanced Marine Vehicle Conference, 78-754, April 1978.

33. Riley, Michael R., Coats, Dr. Timothy W., "The Simulation of Wave Slam Impulses to Evaluate Shock Mitigation Seats for High-Speed Planing Craft," Naval Surface Warfare Center Report NSWCCD-TM-23-2013/26, May 2013.

34. Koelbel, J.G., Jr., "Comments on the Structural Design of High Speed Craft," Marine Technology, Volume 32, No. 2, April 1995, pp. 77-100.

35. Savitsky, Daniel, Koelbel, Joseph, "Seakeeping of Hard Chine Planing Hulls," SNAME, Technical and Research Bulletin No. R-42, June 1993

36. Payne, Peter R., "On Quantizing Ride Comfort and Allowable Acceleration," AIAA/SNAME Advanced Marine Vehicle Conference, paper 76-873, Arlington, VA., September 20-22, 1976.

37. International Standard, "Mechanical Vibration and Shock – Evaluation of Human Exposure to Whole-Body Vibration, Part 1, General Requirements," International Organization for Standardization, ISO 2631-1:1997(E), July 1997.

38. Riley, Michael R., Marshall, Jason T., "Empirical Equations for Developing Ride Severity Envelopes for Planing Craft Less Than 55 Feet in Length," Naval Surface Warfare Center Carderock Division Report NSWCCD-TM-83-2013/36, September 2013.

39. Silfka, Lance, D., "An Acceleration Based Approach to Measuring Displacement of a Vehicle Body," Unpublished master's thesis for master's degree, University of Michigan, Dearborn, Michigan, April 2004.

Distribution

	Copies #
Naval Sea Systems Command PEO Ships, PMS 325G 1333 Isaac Hull Avenue, SE Building 197 Washington Navy Yard, DC 20376 Attn: Christian Rozicer	1
Naval Sea Systems Command TWH Small Boats and Craft 2600 Tarawa Court, Suite 303 Virginia Beach, VA 23459 Attn: Mr. Dean Schleicher	1
Commander Office of Naval Research Sea Platforms and Weapons Division 875 North Randolph Street, Arlington, VA 22203-1995 Attn: Dr. Robert Brizzolara, Code 333	1
Commander Naval Special Warfare Group Four 2220 Schofield Road Virginia Beach, VA 23459 Attn: Sandor Horvath, Code N8	1
United States Coast Guard CG-9 Program Office 2100 Second Street, SW Washington, DC 20593 Attn: Jeff Curtis	1
United States Coast Guard Office of Boat Forces, CG 731 2100 Second Street, SW STOP 356 Washington, DC 20593-7356 Attn: David Shepard	1
United States Coast Guard RDT&E Division 2100 Second Street, SW STOP 7111 Washington, DC 20593-7111 Attn: Frank DeVord	1
Defense Technical Information Center 8725 John J. Kingman Road Fort Belvoir, VA 22060-6218	1

NSWC, CARDEROCK DIVISION
INTERNAL DISTRIBUTION

Code	Name	Copies #
661	Rhonda Ingler	1
8050	Dr. Thomas Fu	1
830	Technical Data Repository	1
831	Willard Sokol, III	1
832	Scott Petersen	1
833	Kent Beachy	1
835	David Pogorzelski	1
835	Kelly Haupt	1
835	Heidi Murphy	1
8302	Dr. Tim Coats	1

NSWC, PANAMA CITY

Code	Name	Copies #
E41	Eric Pierce	1
E23	Brian Price	1
E41	Jeff Blankenship	1

Appendix A. Craft Data Base

The range of significant wave heights, craft average speeds, and craft weights in the database are shown in Figure A1. Accelerometers are routinely installed at stern, LCG, and bow positions, as well as other locations of interest. All acceleration values shown here are from vertical accelerometers positioned at the longitudinal center of gravity. Significant wave heights varied from approximately 2 feet to 6.5 feet, and average speeds varied from 8 knots to approximately 45 knots. Craft displacements in thousands of pounds are illustrated by different colors and symbols. During some of the trials, the coxswains were instructed to operate the craft at the highest possible safe speed for the sea state conditions based on their experienced judgment. Others were run at a pre-determined speed or drive train RPM (i.e., revolutions per minute) as dictated by program requirements.

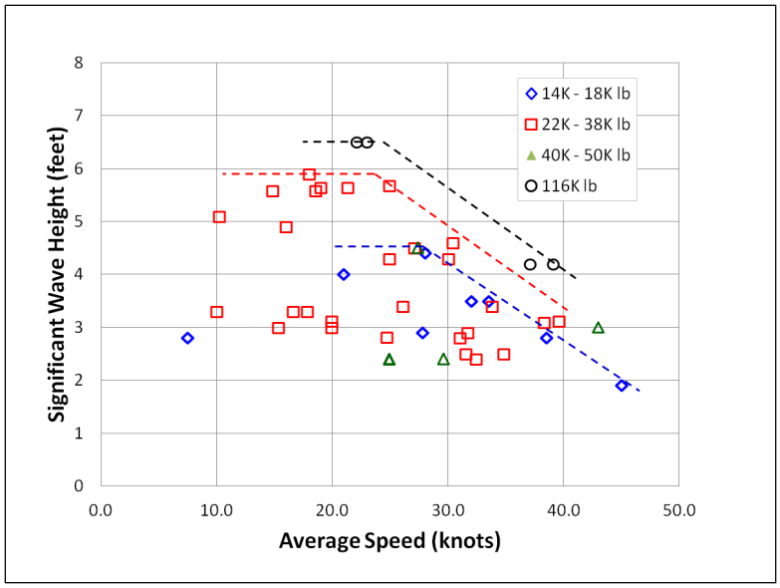

Figure A1. Planing Craft Database

Table A1 compares the range of craft parameters in the full-scale database[6]. The beam loading coefficient is the displacement of the craft divided by the product of the mass density of water and the craft beam cubed. In the last column the speed ratio is craft speed (V_k) divided by the square-root of craft length.

[6] Limited distribution report NSWCCD-23-TM-2012/38, October 2012.

Table A1. Full-Scale and Model-Scale Parameters

Craft Category	Craft Weight (lb)	Beam Loading Coefficient	L/B	Trim (deg)	Deadrise (deg)	$H^{1/3}$ / B	V / $L^{1/2}$	Volume Froude Number
A	14,000 to 18,000	0.28 to 0.46	3.9 to 4.2	3 to 5	18 to 21	0.22 to 0.45	1.2 to 6.1	2.5 to 5.2
B	22,000 to 38,000	0.18 to 0.60	3.0 to 4.2	3 to 5	18 to 22	0.16 to 0.60	1.5 to 5.9	1.8 to4.0

Accelerations recorded vertically at the LCG of each craft were run through the *StandardG* algorithm. Fourier spectra analyses indicated that a 10 Hz low-pass filter was appropriate for extracting the rigid body content.

Seven craft in Category A were deep-V planing hulls (deadrise from 18 to 21 degrees) on the order of 40 feet in length with weights between 14,000 pounds and 18,000 pounds. Testing conditions for this subset of data varied from roughly 21 knots to 45 knots with significant wave heights from approximately 1.9 feet to 4.8 feet. Values of $A_{1/100}$ shown in Figure A2 (in units of g) are estimated within -0.28 g to +0.19 g (i.e., within -7.05% to +6.32%) for 2 g < $A_{1/100}$ < 6.1 g [16]. Values of $A_{1/10}$ shown in Figure A3 for Category A craft are estimated within -6.33% to +3.32% of the data. The gray rectangles are ranges of uncertainty for three $A_{1/100}$ values.

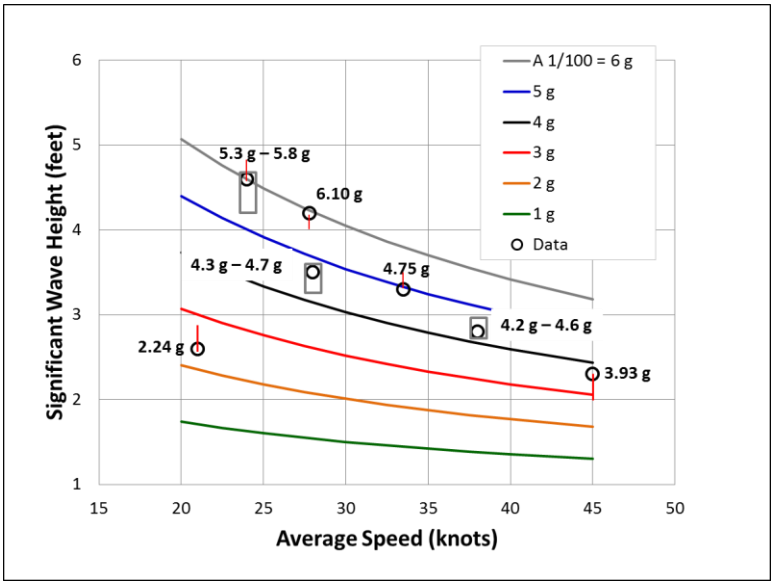

Figure A2. LCG $A_{1/100}$ Data Fit for 14,000 – 18,000 Lb Craft

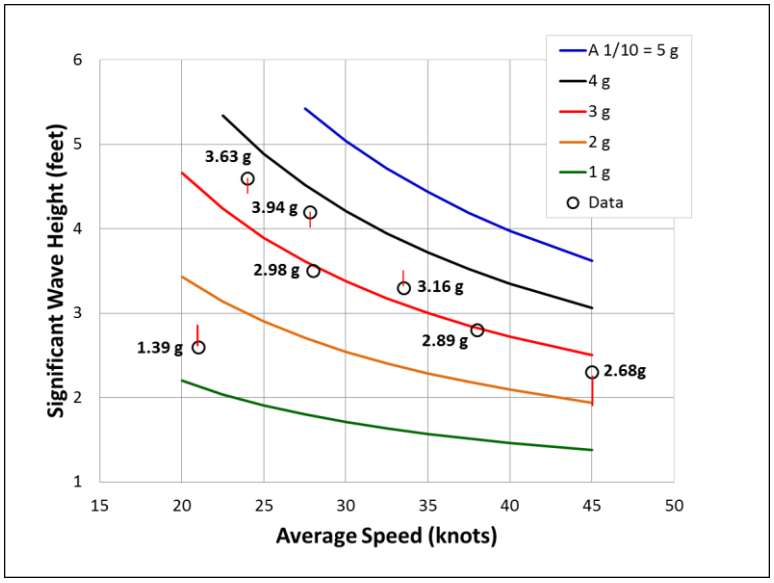

Figure A3. LCG $A_{1/10}$ Data Fit for 14,000 to 18,000 Lb Craft

Eight of ten craft in Category B exhibited discernable $A_{1/100}$ trends during fourteen of sixteen runs. The fourteen runs included significant wave heights ranging from 2.4 feet to 5.7 feet and craft average speeds up to 39.6 knots. V_s is craft average speed in knots, and H is significant wave height in feet. These craft included deep-V planing, as well as one air entrapment hull and a catamaran. Values of $A_{1/100}$ shown in Figure A4 are estimated within -0.25 g to +0.19 g (i.e., -10.50% to +10.70%) for 0.79 g < $A_{1/100}$ < 3.23 g [16]. Values of $A_{1/10}$ shown in Figure A5 at the LCG are estimated for Category B craft within -10.5% to +10.7% of the data.

Discernable peak acceleration trends with the volume Froude number were not observed in this limited data set.

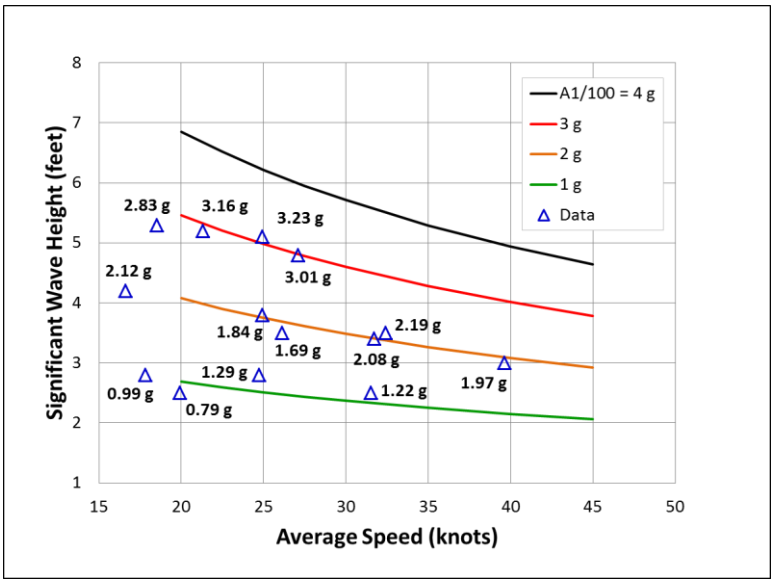

Figure A4. LCG $A_{1/100}$ Data Fit for 22,000 – 38,000 Lb Craft

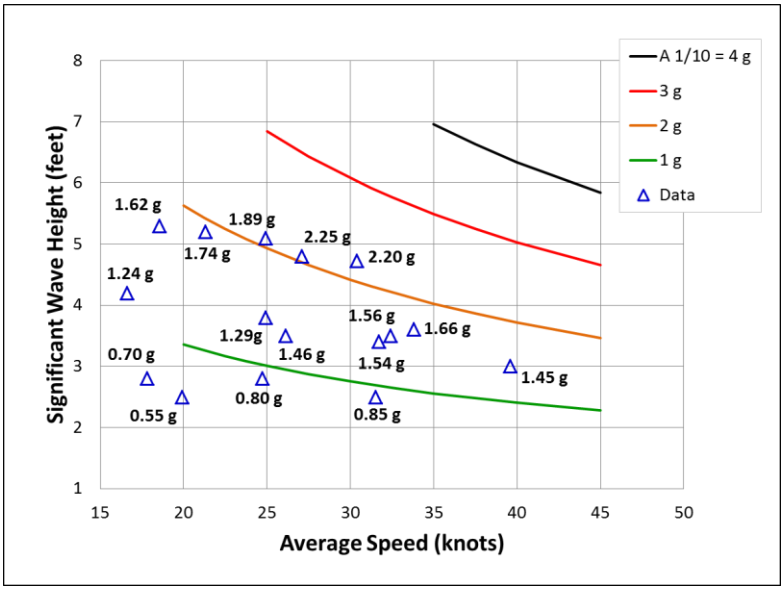

Figure A5. LCG $A_{1/10}$ Data Fit for 22,000 – 38,000 Lb Craft

Based on a sensitivity analysis of the individual data points within the database, it was assumed that average craft speeds may vary on the order of +/- 3 knots, and published significant wave heights from wave buoy data may vary on the order of +/- 6 inches depending upon the location of the buoy relative to the craft's actual position during seakeeping trials. The lines shown in the data plots should therefore be used to indicate transition zones rather than hard lines that yield exact numbers.

For all runs with from 303 to 621 peak accelerations greater than the RMS acceleration the ratio of the maximum peak acceleration to the A1/100 value is given by equation (A1). A_{max} is

the largest of all A_{peak} values for a given run. The ratio for 18 of 21 data points were less than 1.2.

$$1.06 \leq \frac{A_{MAX}}{A_{1/100}} \leq 1.47 \qquad \text{Equation (A1)}$$

As shown in Figure A6, for a given peak acceleration amplitude, a range of duration time values is observed in the data base. The scatter in the data is likely due to several variables, including craft weight, speed, wave height, impact angle, deadrise, and where the craft impacted a wave (e.g., on the leading flank, crest, or following flank). For example, for the lighter weight craft (blue circles), when the peak acceleration was 3 g, the impact durations varied from approximately 110 milliseconds to 200 milliseconds. The dotted lines in the figure are the upper bound of the range of values for each craft weight category. Equation (10) is the blue dotted line for category A craft, and equation (13) is the red dotted line for Category B craft. The figure is a compilation of observations from detailed analyses of only the more severe wave impacts in the trials data. Duration times for Category A craft impacts with peak accelerations less than 2 g are not plotted, but the shortest observed duration is on the order of 100 milliseconds except for one data point.

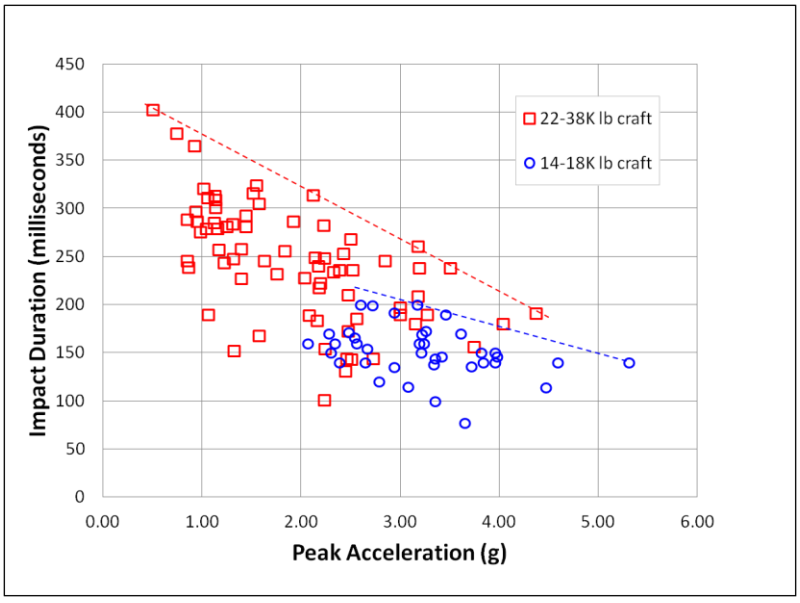

Figure A6. Impact Duration versus Peak Acceleration

Appendix B. Wave Impact Change in Velocity

Direct Integration

One approach to estimating the change in velocity that occurs during a wave impact is to integrate the acceleration record. The other approach is to use A_{max} and T for individual wave impacts. The change in velocity for a half-sine pulse can then be calculated using equation (7) in the main body of the report.

Two numerical problems may be encountered when integrating acceleration time histories. First, there may be drift in the calculated velocity plot that is caused by very low frequency content (referred to as direct current bias) in the acceleration signal. Second, the constant of integration is seldom known [39]. To remove the DC bias the record should be demeaned to ensure that the average acceleration amplitude of all the data points in the record is zero, and then a low frequency high-pass filter (e.g., 0.025 Hz high-pass filter) should be applied. This approach yields velocity time histories as shown in Figure B1. The constant of integration (i.e., the initial velocity at time zero) is also not known. One approach to minimizing this uncertainty is to demean the velocity record prior to applying the peak extraction algorithm [39].

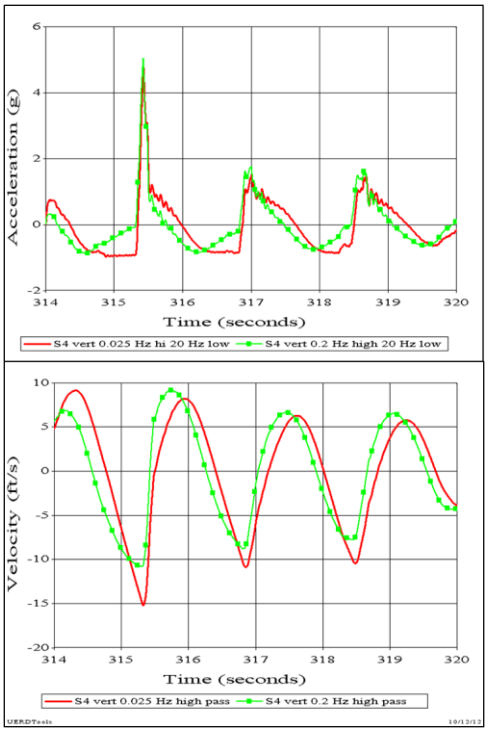

Figure B1. Effect of High-Pass Filter on Acceleration and Velocity

The current practice of using a 0.025 Hz high-pass filter is based on recent experience while processing craft seakeeping data[7]. It has been observed that the peak velocity values for individual wave impacts are significantly reduced (for records that are longer than four minutes in length) when the high-pass filter amplitude is increased up to 0.2 Hz. Figure B1 shows this effect by comparing a 0.2 Hz high-pass filtered record (green curve with circles) with one processed using a 0.025 Hz high-pass filter (red curve). The distorted free-fall period in the green acceleration curve prior to each wave impact significantly reduces the area under the acceleration time history, which distorts the peak velocity. The velocity plot shows how each negative peak velocity prior to each impact is reduced. For example, the impact velocity for slam 315 is incorrectly reduced from 15.2 fps to 10.8 fps. The physics-based criterion for high-pass filtering is that the free-fall period should not be altered in such a way that significantly diminishes the impact velocity.

Figure B2 shows the decrease in the peak impact velocity with increasing high-pass filter amplitude. The plot includes data from twenty-six wave impacts recorded on nine different craft. The data includes accelerations recorded at bow and LCG locations. The decrease is not the same for different acceleration histories, but review of many acceleration time histories indicates that the 0.025 Hz high-pass filter results in less than a three percent decrease in peak impact velocity. The plot shows that when the high-pass filter is reduced to 0.01 Hz spurious jumps (i.e., impact velocity decrease) occur in some data sets that should be avoided. Selection of the high-pass filter rate for other data should be based on ensuring little or no change in constant -1 g free fall events (i.e., no reduction in impact velocity) and analysis of the acceleration record Fourier spectrum.

Figure B3 shows an eight second sample of unfiltered and 10 Hz low-pass filtered vertical accelerations plotted with the corresponding velocity time histories obtained by direct integration. The accelerometer was located at the longitudinal center of gravity (LCG) of the craft. The grey acceleration curve is the unfiltered acceleration that contains both the rigid body and local vibration components. The black rigid body acceleration curve was obtained by subjecting the unfiltered curve to a 10 Hz low-pass filter to remove the vibration content.

Both curves in Figure B3 show three severe wave impacts with much steeper rise times and larger peak accelerations than the other four lower severity wave encounters. The three largest wave slams are numbered according to the time in seconds when the impact occurred. For example, slam 193 occurred at or after the 193-second point in time. The forced local vibrations due to each impact are observed in the acceleration record to damp out before the next wave impact; therefore each wave impact can be analyzed as a single dynamic input and a corresponding dynamic response.

The grey and black velocity curves in Figure B3 (lower plots) are almost indistinguishable. The grey velocity curve was generated by integrating the unfiltered acceleration curve, and the black velocity curve (with circles) was created by integrating the 10 Hz low-pass filtered acceleration curve. A drift correction process was applied to both curves to remove velocity drift introduced in the integration process and they were demeaned. Each curve provides an estimate of the absolute rigid body velocity at the LCG in the vertical direction. The two curves are not

[7] Limited distribution report NSWCCD-23-TM-2012/36, September 2012.

exact, but they are very similar. They demonstrate that the integration process is a natural filtering process that removes higher frequency acceleration oscillations [39].

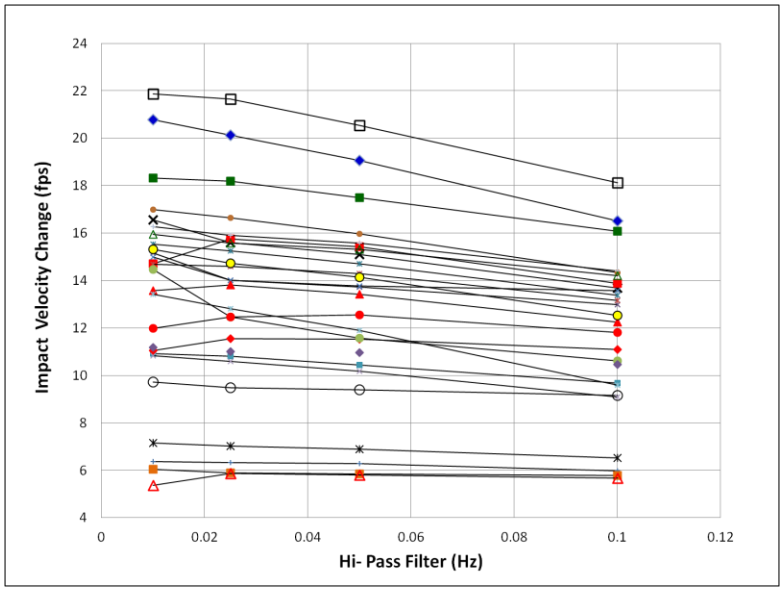

Figure B2. Effect of High-Pass Filter on Impact Velocity

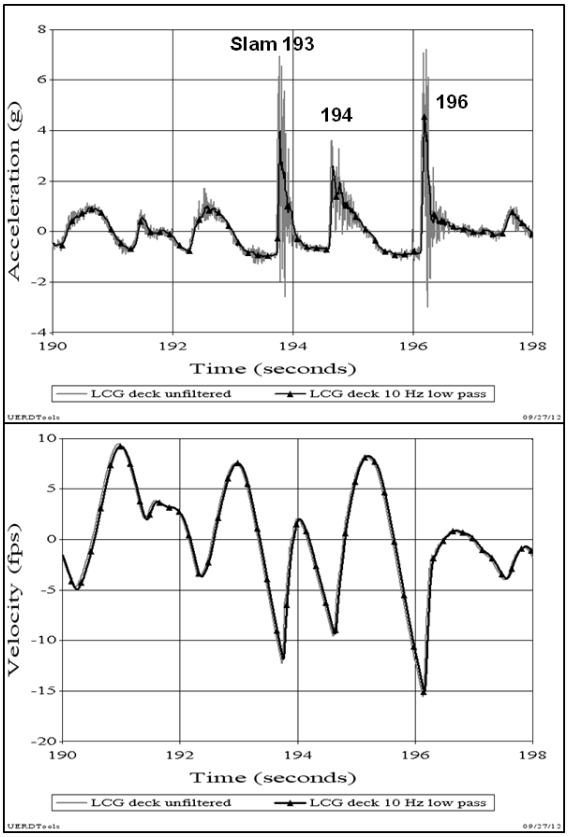

Figure B3. Acceleration and Velocity Time Histories

In Figure B3 each wave impact begins with the negative velocity dip (i.e., curve minimum) and the impact ends when the velocity returns to zero. The change in velocity during the impact period is equal to the maximum negative velocity just before impact. Table B1 indicates that the largest negative velocities from the unfiltered acceleration record are within plus or minus four percent of the velocity obtained from the low-pass filtered acceleration.

Table B1. Effect of Low-Pass Filtering on Velocity

Slam Number	Velocity Change (fps)		
	Unfiltered	10 Hz low pass	Percent Difference
190	4.73	4.95	-4.36
192	3.66	3.69	-0.52
193	12.24	11.82	3.55
194	9.57	9.31	2.87
196	15.56	15.08	3.18

For wave slam 193, the free fall period prior to the impact results in a negative velocity (i.e., motion downward) of about -12 fps just prior to impact (grey curve), and it takes approximate 0.156 seconds for the velocity to increase to zero. During this period the rigid body acceleration increases from -1 g to a peak of about +3.9 g, and returns to about +1g within the 0.156 second impact period. The peak acceleration is the instantaneous point in time where the slope of the velocity curve is a maximum, and it is proportional to the net upward force acting at the LCG at that instant in time. In this example the velocity of the craft goes from -12 fps to zero during the impact period, for a net change in velocity of +12 fps. With this additional information, we can characterize the wave slam load as an impulsive load of 0.156 seconds duration that caused a sudden change in velocity of +12 fps and a peak rigid body response acceleration of 3.9 g. In a similar fashion, slams 194 and 196 result in velocities of 9.5 fps and 15.5 fps, respectively. The magnitude of the peak negative velocity just before impact is therefore a measure of the severity of the wave impact load. The order of severity for the three wave slams based on velocity is slam 196, 193, and 194 (i.e., 15.5 fps, 12.0 fps, and 9.5 fps). The inference is that the potential for damage at 15.5 fps is more than the damage potential at 9.5 fps. This is also the same rank ordering of severity in terms of peak acceleration (4.5 g, 3.9 g, and 2.5 g).

The impact velocities and peak accelerations from the data can be used to compute the estimated impact duration for a half sine pulse using equation (7). For slams 193, 194, and 196 the computed durations are 0.153 sec, 0.186 sec, and 0.168 sec.

List of Sorted Peak Velocity

Figure B4 shows a velocity time history obtained by integrating an acceleration record that was first subjected to a 0.025 Hz high-pass filter. The change in velocity for each wave impact is seen as the negative peaks. The impact velocity change for each impact can be extracted automatically from the record by applying the same algorithm used to extract peak accelerations.

The velocity time history shown in Figure B4 was inverted by multiplying the amplitude of the entire curve by minus one. The negative peaks then became positive peaks. The inverted velocity record was then subjected to the *StandardG* algorithm to extract the positive peaks. The same 0.5 second horizontal criteria can be used, but a vertical threshold value had to be selected to establish a velocity level above which to count velocity peaks. When the *StandardG* algorithm was applied to the original acceleration time history, a list of 156 peak accelerations greater than the RMS acceleration was obtained. It was determined by tedious trial and error that a threshold value of RMS velocity divided by four yielded 156 peak velocities. The same number of velocity and acceleration peaks (i.e., 156 in this case) was used as an interim rationale for extracting peak velocity values from the record in Figure B4.

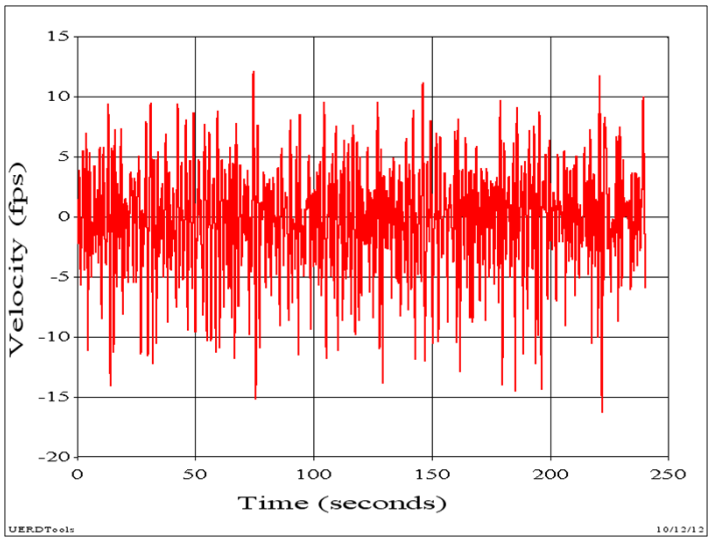

Figure B4. Example Velocity Time History

Figure B5 shows the plot of peak impact velocities extracted by the *StandardG* algorithm from the inverted velocity curve. It shows the 156 values (i.e., values greater than the RMS velocity divided by 4) plotted largest to smallest. $V_{1/100}$ is16.2 fps, $V_{1/10}$ is 13.2 fps, $V_{1/3}$ is 10.8 fps, V_{avg} is 6.8 fps, and V_{RMS} is 4.1 fps.

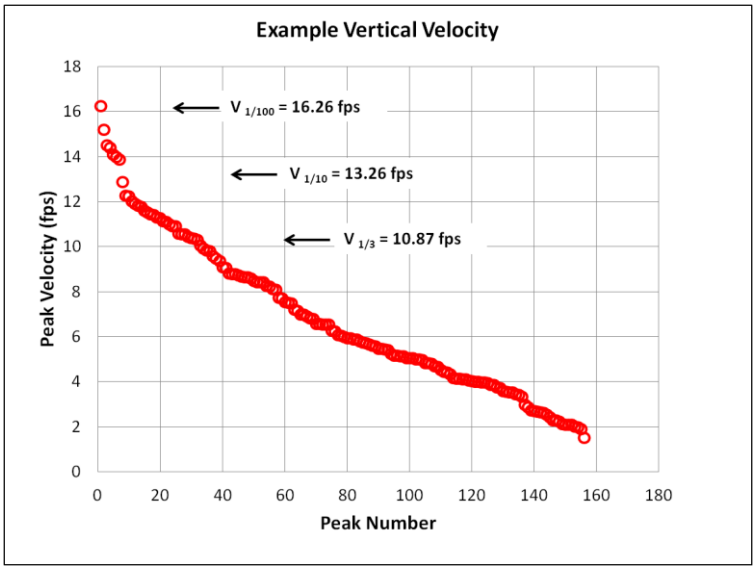

Figure B5. Impact Velocity Sorted Largest to Smallest

The $V_{1/N}$ values listed in Figure B5 were obtained based on a velocity threshold criterion that provides the same number of peak velocities as peak accelerations (i.e., N=156). Although this approach has intrinsic merit, it resulted in a tedious iterative process to find the velocity threshold that yielded N=156. In this example it was approximately V_{RMS} divided by four. Subsequent study of other acceleration data showed no consistency in the threshold criterion based on equating the number of peak velocities to the number of peak accelerations.

In order to pursue a less tedious computational process a vertical threshold criterion equal to the RMS velocity of the velocity time history was investigated. Velocity time histories for fourteen different craft were developed by integrating an acceleration record that was filtered with a 0.025 Hz high-pass filter. Values of $V_{1/100}$, $V_{1/10}$, $V_{1/3}$, V_{AVG} and V_{RMS} were computed using the *StandardG* algorithm for two threshold values. One threshold value was equal to the RMS velocity (Threshold = RMS velocity), and the other was the velocity that yielded the same number of peaks as the acceleration peaks (Threshold = N). Computed $V_{1/N}$ velocity values vary from roughly 1 fps to 20 fps. The results are plotted in Figure B6 where the blue-dotted line has a slope of 1.0. The computed $V_{1/100}$, $V_{1/10}$, $V_{1/3}$, and V_{AVG} values were all larger when the threshold was chosen to be equal to the RMS velocity. The V_{AVG} and $V_{1/3}$ values are up to 1.18 times the Threshold equal N values or less. The $V_{1/100}$ and $V_{1/10}$ values are approximately 1.05 times the values for equal N (except for one V1/10 velocity value equal to 11 fps).

The abscissa in Figure B6 also shows the equivalent drop test heights that result in a given value of impact velocity. For example, an impact velocity of 20 fps corresponds to a drop height of about 6 feet, and 10 fps corresponds to about 1.5 feet.

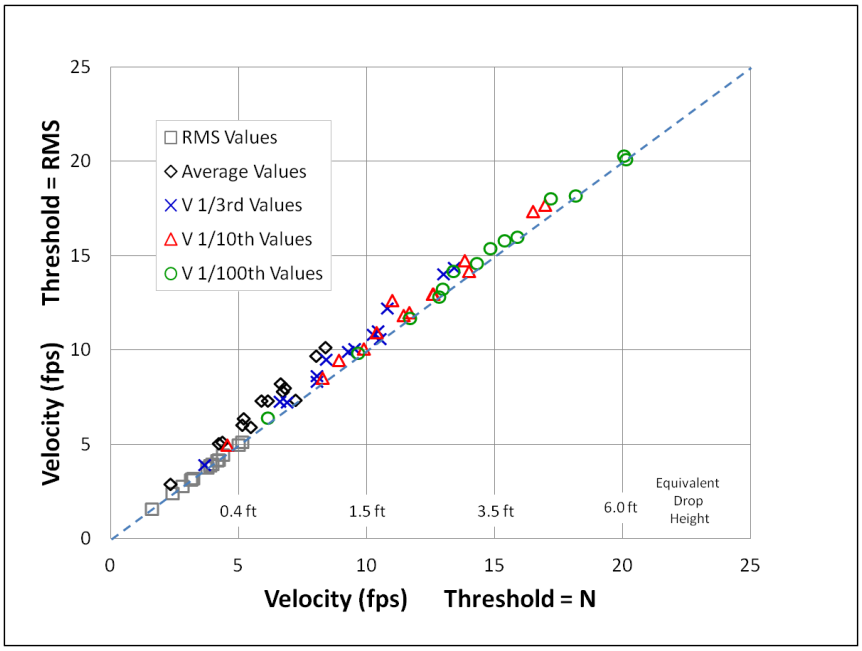

Figure B6. Average and RMS Velocities for Two Threshold Criteria

When the RMS velocity is selected as the threshold value for extracting peak velocities, the tedious iterative process is eliminated, and the computed $V_{1/100}$ and $V_{1/10}$ values are less than five percent larger than when the threshold is equal N. It is therefore recommended that the RMS velocity value be used as a threshold value when computing $V_{1/N}$ values. This results in computational processes for both peak accelerations and impact velocities based on RMS threshold criteria.

This page intentionally left blank


NAVSEA
WARFARE CENTERS
Carderock